A STUDY OF THE NEUTRAL DECAY

BRANCHING RATIOS OF THE ETA MESON

by

Bruce A. Nelson

B.S., M.I.T.

(1961)

SUBMITTED IN PARTIAL FULFILLMENT

OF THE REQUIREMENTS FOR THE

DEGREE OF DOCTOR OF

PHILOSOPHY

at the

MASSACHUSETTS INSTITUTE OF

TECHNOLOGY

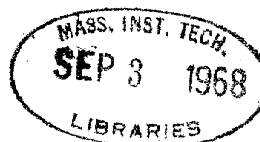August, 1968, *i.e. 1969*

Signature of Author_____

August 21, 1968

Certified by_____

Thesis Supervisor

Accepted by_____

Chairman, Departmental Committee
on Graduate Studies

A STUDY OF THE NEUTRAL DECAY

BRANCHING RATIOS OF THE ETA MESON

by Bruce A. Nelson

SUBMITTED IN PARTIAL FULFILLMENT OF THE REQUIREMENTS

FOR THE DEGREE OF DOCTOR OF PHILOSOPHY

August 21, 1968

ABSTRACT

This work reports a determination of the decay branching ratios of the eta meson into 2γ, $\pi^0\gamma\gamma$, and $3\pi^0$ assuming that no other neutral modes are relevant. The etas were produced in the reaction $\pi^- + p \rightarrow \eta^0 + n$ with an incident momentum of 752.5 MeV/c. The data is consistent with there being no $\pi^0\gamma\gamma$ decay mode of the eta. The branching ratios are

$$R(2\gamma/3\pi^0) = 1.41 \pm 0.22$$
$$R(\pi^0\gamma\gamma/2\gamma + 3\pi^0) = -0.13 \pm 0.13$$

Thesis Supervisor: Lawrence Rosenson

Title: Professor of Physics

ACKNOWLEDGMENTS

OUTLINE

INTRODUCTION

Until recently considerable uncertainty existed in the determination of the branching ratios of the eta meson into its various modes particularly the neutral modes. The purpose of the experiment described in this thesis was to improve the determination of the branching ratios of the eta meson. Only the determination of the neutral branching ratios of the eta will be discussed in this thesis.

The eta meson was discovered by Pevsner et al (1) in a study of the invariant mass of the three pions produced in the reaction $\pi^+ d \rightarrow pp\pi^+\pi^-\pi^0$. The invariant mass distribution of the three pions showed an accumulation of events in the region of 550 MeV. A phase space distribution of the invariant mass of the three pions showed no such accumulation in the same region. The accumulation of events was attributed to the existence of a particle, called the eta meson, with a mass of approximately 550 MeV.

The latest value of the mass of the eta from Rosenfeld et al (2) is 548.8 $\pm$ 0.6 MeV. The measurement of the width of the eta has, so far, been limited by the resolution of the experiment. The width is believed to be very narrow ($\sim$1 kev). The quantum numbers of the eta are well established as $T = 0$, $J^{PG} = 0^{-+}$ (3)(4)(5)(6).

The principle neutral decay modes of the eta which are allowed by the known conservation laws are

$$\eta^0 \rightarrow \begin{cases} 2\gamma \\ \pi^0\gamma\gamma \\ 3\pi^0 \end{cases}$$

Since the $3\pi^0$ decay violates G-parity, it must result from an electromagnetic interaction as do the 2γ and $\pi^0\gamma\gamma$ decays.

At the present there are very few theoretical works which predict the neutral branching ratios. It is difficult to understand theoretically the observed ratio of the 2γ to $3\pi^0$ modes. Both of these decays are electromagnetic and so are proportional to α^2 where α is the fine structure constant. However, since the two body decay has much more phase space available than the three body decay, the 2γ mode should completely dominate the $3\pi^0$ mode. Instead, the observed ratio of these two modes is of the order of unity.

One possible solution to this dilemma has been proposed by Bronzan and Low (7). They suggested the existence of a new quantum number called the A quantum number. The eta and pi mesons were assigned the value A = -1 and gammas were assigned the value A = +1. On this basis the 2γ decay of the eta is A forbidden but the $\pi^0\gamma\gamma$ decays are A allowed. This would suppress the 2γ mode compared to the $\pi^0\gamma\gamma$ or $3\pi^0$ modes. One would then expect to see approximately equal contributions from all the neutral modes.

Introducing a two-photon-pseudoscalar-meson interaction and a direct four-pseudoscalar-meson interaction into Schwinger's field theory of matter Chan (8) is able to predict the neutral branching

ratios of the eta. His predictions are $2\gamma/3\pi^0 = 1.07$ and $\pi^0\gamma\gamma/$
$2\gamma + 3\pi^0 = 0.04$.

Van Royen and Weisskopf (18) use a quark model to make predic-
tions about several meson decays. In this model they construct the
vector and pseudoscalar mesons from S states of quark-antiquark sys-
tems. On the basis of their model they predict that the ratio of
$\eta^0 \rightarrow \pi^0\gamma\gamma$ to $\eta^0 \rightarrow 2\gamma$ should be 0.0005.

The past experiments which have observed the neutral modes of
the eta seem to fall into two groups. One group of experiments which
we shall refer to as the old experiments found that the $\pi^0\gamma\gamma$ decay mode
accounted for roughly 20% of the total eta decays. The other group
of experiments which we shall call the new experiments found little
or no $\pi^0\gamma\gamma$ decay. We present a compilation of previous work in the
following table. For each experiment the observed decay modes are
given as a fraction of the total neutral decay modes unless otherwise
stated.

Old experiments

Di Giugno et al. (9)

$2\gamma = 0.416 \pm 0.022$ $\pi^0\gamma\gamma = 0.375 \pm 0.036$ $3\pi^0 = 0.209 \pm 0.027$

Grunhaus(10)

$2\gamma = 0.440 \pm 0.070$ $\pi^0\gamma\gamma = 0.270 \pm 0.100$ $3\pi^0 = 0.290 \pm 0.100$

Feldman et al. (11)

$2\gamma = 0.579 \pm 0.052$ $\pi^0\gamma\gamma = 0.244 \pm 0.050$ $3\pi^0 = 0.177 \pm 0.035$

New experiments

Buniatov et al. (12)

$2\gamma = 0.590 \pm 0.033$ $\pi^0\gamma\gamma < 0.12$ $3\pi^0 = 0.410 \pm 0.033$
                                        (95% confi-
                                        dence level)

Jacquet et al. (13)

$\pi^0\gamma\gamma$ / all decays < 0.120 (90% confidence level)

Baltay et al. (14)

$2\gamma = 0.533 \pm 0.046$ $\pi^0\gamma\gamma < 0.150$ $3\pi^0 = 0.467 \pm 0.067$
                                        (95% confi-
                                        dence level)

Wahlig et al. (15)

$\pi^0\gamma\gamma < 0.500$ (90% confidence level)

In addition Chretien et al. (5) found $2\gamma/3\pi^0 > 0.9$ and Cence et al. (16)

found $2\gamma/3\pi^0 = 0.9 \pm 0.2$. A compilation of the results of several

experiments presented at the 1967 Heidelberg Conference (17) gives

$2\gamma = 0.562 \pm 0.037$ $\pi^0\gamma\gamma = 0.027 \pm 0.027$ $3\pi^0 = 0.411 \pm 0.032$

which gives ratios of

$R(2\gamma/3\pi^0) = 1.367 \pm 0.139$ $R(\pi^0\gamma\gamma/2\gamma + 3\pi^0) = 0.0003 \pm 0.0003$

Rosenfeld et al. (2) have fit the data from both the old and new ex-

periments to obtain the best values for the neutral decay modes. They

found for the old experiments

$2\gamma = 0.479 \pm 0.040$ $\pi^0\gamma\gamma = 0.268 \pm 0.045$ $3\pi^0 = 0.254 \pm 0.044$

and for the new experiments

$2\gamma = 0.592 \pm 0.042$ $\pi^0\gamma\gamma = 0.014 \pm 0.026$ $3\pi^0 = 0.394 \pm 0.047$

The ratios for the old experiments are

$$R(2\gamma/3\pi^0) = 1.886 \pm 0.362 \qquad R(\pi^0\gamma\gamma/2\gamma + 3\pi^0) = 0.366 \pm 0.067$$

The ratios for the new experiments are

$$R(2\gamma/3\pi^0) = 1.503 \pm 0.208 \qquad R(\pi^0\gamma\gamma/2\gamma + 3\pi^0) = 0.014 \pm 0.024$$

THE EXPERIMENT

Introduction

This experiment was conducted at the B.N.L. Cosmotron. The experimental setup and apparatus are shown in Figs. 1, 2, and 3. The experiment was designed to measure the ratios of the various decay modes, both charged and neutral, of the eta meson. This thesis deals with the neutral modes.

The eta mesons were created by the interaction of a momentum selected pi minus beam with protons in a liquid hydrogen target. Surrounding the target on four sides were two sets of four nested spark chambers. The inner set was used for detecting charged prongs and the outer set for converting gamma rays into electron-positron pairs. In this thesis the term gamma ray will usually mean the electron-positron pair created by the conversion of a gamma ray.

The neutron which was produced in the interaction was detected by a neutron detector composed of a series of scintillation counters and spark chambers centered on an angle of 20° to the beam line. The angle was chosen to take advantage of the kinematics of neutrons produced in the reaction $\pi^{-} + p \rightarrow \eta^{\circ} + n$. At our beam energy most of the neutrons were produced at angles close to 20°.

The front of the neutron detector was approximately 3 m. from the hydrogen target. At the front, the detector covered an angular region of 5° in polar angle from 17.5° to 22.5° and it subtended 1/13 of the azimuth. The length of the detector was 1.25 meters.

A picture was taken whenever the electronic logic detected a beam

particle interacting in the target and producing a neutral particle which interacted in the neutron detector. The time-of-flight of the neutral particle was also measured. For our apparatus the time-of-flight of neutrons ranged from 26 to 42 nanoseconds.

Beam

The incident beam in this experiment was composed of negative pions created in a copper target placed at the focus of the external proton beam from the Cosmotron. The copper target was placed in front of magnet B1 (see Fig. 1). The pions were extracted at an angle of 7° to the proton beam. Magnet B2 bent the pion beam through 20° which provided the necessary momentum selection. The quadrupole magnets Q1 and Q2 focused the beam on a 1 cm. slit located downstream from magnet B2. The slit gave a momentum resolution of 1.3 percent full width. After collimation the beam was pitched up to a height of approximately 100 inches above the floor. The quadrupoles Q3 and Q4 focused the beam on the hydrogen target and the B3 bent the beam so that it was incident horizontally on the target.

The central value of the beam momentum was determined by placing a calibrated Hall probe inside magnet B2 and monitoring its current and voltage throughout the run.

The momentum loss by the beam due to its passage through the counters and spark chambers in front of the target was calculated to be 10.5 MeV/c.

Target

    The target consisted of a mylar shell, approximately spherical in shape with a diameter of 4 cm. and a thickness of 0.002 inches, which was filled with liquid hydrogen. The target was gravity fed from a reservoir located directly above it and thus was kept filled at all times during the run. The target was surrounded by a vacuum jacket made of mylar on an aluminum framework which was attached to the bottom of the reservoir.

Counter Logic

The positions of the scintillation counters used for the electronic logic are shown in Figs. 2 and 3. Counters 1 and 2 were beam defining counters. Counter 3', a large anti-counter with a beam hole, was used to anti out misaligned beam particles and products from beam particles which interact upstream. Counter 3 was a final beam defining counter. Counters 4 and 4' were anti-counters which were used to anti out beam particles passing through the target. Counters 5 and 5', 6, 7, 8, and 9 formed an anti-counter shield in front and on the beam side of the neutron detector.

The electronic logic had two functions to perform. First it had to decide when to trigger the spark chambers and take a picture and second, it had to determine the neutron's time-of-flight. A brief description of these two functions follows. For a more complete description see Appendix A .

The first requirement for a good trigger was that the beam particle interact in the target. Such an occurrence gave the signature $123\bar{3}'\bar{4}\bar{4}'$. The second requirement was that at least two adjacent counters in the neutron detector gave signals which were in coincidence and also that the coincident signal was in a certain time region with respect to the beam particle. Finally, there was the requirement that no signal come from any of the counters in the anti shield around the neutron detector.

When all these requirements were met, we knew that the beam particle

interacted in the target, that the neutron detector was triggered as the result of a neutral particle interacting in the detector, that the timing was such that the neutral particle was probably a neutron, and that the recoil which resulted from the interaction of the neutral particle must have passed through at least one spark chamber. At this point the spark chambers were triggered and a picture was taken.

The neutron time-of-flight was determined by measuring the overlap between the coincidence signal from a pair of neutron detector counters and a reference signal from counter 1 using a time-to-pulse-height converter. The signals from the coincidence circuits for the different pairs of neutron detector counters were all fanned into one line. Therefore the pair of counters which gave the timing signal was the pair whose coincidence signal arrived at the fan-in first. The logic was arranged so that fast neutrons gave signals which had more overlap with the reference signal than slow neutrons. Since there was a direct corresponence between overlap and pulse height, fast neutrons gave bigger pulses than slow neutrons.

The output from the time-to-pulse-height converter was fed into the analog-to-digital circuitry which was, in effect, a 256 channel pulse-height analyzer. This circuitry converted the pulse height into a channel number between 0 and 255. The channel number was recorded on the film in binary lights called A-D lights.

Main Array

The main array consisted of two sets of four nested spark chambers. Each set of chambers was nested to form a box with the top and bottom open. The inner set of chambers consisted of four-gap, thin-foil spark chambers which were used to detect charged prongs coming from the target. The outer set of chambers was used to detect gamma rays and to give an indication of the range of those charged prongs which passed through the inner chambers (see Fig. 2).

The array of the four outer chambers is described in detail in Ref. (19). Each chamber consisted of fifty, square steel plates, 75 cm. on a side and 2 mm. thick, which is equivalent to 5.5 radiation lengths of steel. This was sufficient to convert into electron-positron pairs practically all of the gamma rays which struck the chambers. The gap width between chamber plates was 3 mm. so when the chamber was assembled it was approximately 25 cm. thick.

Each high voltage plate was driven by its own spark gap and con-denser in an attempt to provide good efficiency for detecting multiple tracks by cutting down on one track robbing another. Approx-imately forty nanoseconds after the high voltage was applied to the chamber plates the excess voltage on all undischarged gaps was dumped to ground thus preventing any spurious sparking in the chambers.

A circular hole 3.5 inches in diameter was cut in the upstream outer chamber to allow the beam to pass through the chamber without interacting. Aluminum foil patches were applied to five plates in

the front and back of the chamber so that sparks giving the location

of the beam track could be seen in four gaps at the front and back

of the chamber. A rectangular hole 4 inches by 3.75 inches was cut

in the downstream outer chamber. The center line of the hole

made an angle of 20° with the beam line. The holes in the individual

plates were covered with aluminum foil which allowed tracks to be

visible in the region of the hole but presented little material

for neutrons coming from the target to interact in. This prevented

neutrons from interacting before they reached the neutron detector.

Each chamber was seen in 90° stereo. An arrangement of mirrors

allowed both the direct and side views of all chambers to be seen by

one camera.

The small inner chambers surrounded the target on four sides.

They were constructed by placing two sheets of one mil aluminum foil

on a 12 inch by 7 inch aluminum frame to form one plate. Five plates

were held together by lucite spacers which gave a gap size of 0.25 inches.

The amount of material in the chambers was kept small enough so that

the chance of a gamma ray converting before reaching the outer chambers

was minimal.

Neutron Detector

The neutron detector was composed of a series of scintillation counter-spark chamber sandwiches. Each sandwich was composed of a scintillation counter, then a two-gap, thin-foil spark chamber, then another counter. There were twenty spark chambers and twenty-one scintillation counters in all. The counters were 26 cm. by 45 cm. by 2.5 cm. and the spark chambers were 30 cm. by 90 cm. with two 7 mm. gaps. Two views of the neutron detector are shown in Fig. 3.

The neutron detector was centered on a line which made an angle of 20° with the incident beam line. It was covered in front and on the beam side by an anti-counter shield. Neutrons coming from the target interacted in one of the scintillators producing a proton recoil. At the minimum the recoil was required to pass through the spark chamber and into at least the next counter or else no picture was taken. It may, of course, have gone further before leaving the detector or stopping.

The thickness of the scintillation counters was chosen on the basis of preliminary studies made at the Cosmotron. A portion of the neutron detector consisting of three counters and two spark chambers was used to study the neutron detection efficiency as a function of the counter thickness. Based on this study the counter thickness was chosen as 2.5 cm.

Attached to the neutron detector frame were two sheets of lucite, one for the side view and one for the direct view. On these sheets were

ruled lines which defined the edges of the scintillation counters in each view. The lines were illuminated whenever a picture was taken so that they would be visible on the film.

The location of the counters in each view was marked by Sylvania electroluminescent panels which were attached to the lucite sheets. The panels were approximately as wide as the counters were thick so none of the spark chambers were blocked from the camera view. When an event was detected by the electronic logic, the panels which marked those counters giving signals were illuminated. This made it possible to know which counters had given signals for each event. Once the counters which gave signals were known, it was then possible to determine which counter pair gave the timing signal and from this information, to determine the neutron time-of-flight (see Appendix B).

The neutron detector was seen in 90° stereo. Mirrors were arranged so that the two views of the neutron detector were seen by the same camera which photographed the main array.

Photography

The main array and the neutron detector were enclosed in a light-tight, concrete block house so that the camera could be operated with its shutter always open. The camera used in this experiment was a Richardson 70 mm. camera. The film was sprocketed film which was advanced after each event. The mirror arrangement was such that all views of the main array and the neutron detector were seen by one camera.

Besides the views of the main array and the neutron detector the pictures contained the roll and frame number, the lights giving the neutron time-of-flight, and fiducial lights for each chamber. There were two types of fiducial lights. One was used for determining the various parameters associated with the geometric reconstruction such as the camera location for each view or the transformation from one chamber system to the main coordinate system. The other type was used in the geometric reconstruction itself such as the fiducial crosses which were seen in the side views of the outer chambers and were used to establish the transformation to the normalized film plane. For a complete discussion of the method of the geometric reconstruction see Ref. (20).

DATA REDUCTION

Scanning

The scanning procedure was simplified by the introduction of
several cuts which could be made on the scanning table and which
eliminated the necessity of examining each picture in detail. It
was found during preliminary analysis of the data by the group
from Padova University in Italy that for good eta events only one
or two counter pairs in the neutron detector gave signals. It was
decided on the basis of this information to eliminate from our
sample all those events with more than four consecutive lights on
in the neutron detector. Also the time-of-flight of a neutron pro-
duced with an eta gave a reading of less than 160 in the analog-
to-digital (A-D) lights so those events which had A-D lights greater
than 160 were eliminated.

Those pictures which remained after the application of the cuts
were given an event code and classified as to type. The type of
event was a description of what was in the picture, for example four
gammas or two charged prongs and two gammas were event types. The
event code was a two-digit number describing the general condition
of the main array and the neutron detector. The first digit described
the main array and the second digit described the neutron detector.
The event code determined whether or not a picture was measured.
A list of the possible codes for the main array and the neutron de-
tector follows. During the following discussion the outer set of
spark chambers are referred to as the large chambers and the inner set

as the small chambers.

Main Array Codes

0 --- Good trigger

1 --- A good trigger with one extra beam track

2 --- A good trigger with one extra beam track which interacts in one of the large chambers

3 --- Only straight through tracks are visible

4 --- A possible good trigger with more than one extra beam track

5 --- Upstream interaction

6 --- Downstream interaction

7 --- Beam track was absent in the upstream large chamber

8 --- Neutron recoil or star in a large chamber

9 --- Trash which fits no other category

A code of 0 was given to events where a well defined beam track interacted in the target. A well defined beam track was one which had at least one spark in the upstream large chamber and a spark in the upstream small chamber gap closest to the target. This was the minimum requirement. Usually the beam track had more than two sparks. The maximum it could have was six.

A code of 1 was given to events where the picture contained one extra beam track which did not interact in the target. Usually these were beam tracks which passed through the main array during the

approximately 200 nanosecond delay between the time when it is decided
to take a picture and the actual firing of the spark chambers. For
the most part these extra beam tracks caused no confusion in identi-
fying the beam track responsible for the event. In those cases where
there was an extra beam track in the small chambers and that track
had a spark in the gap closest to the target the interacting beam
track was not required to have a spark in that gap since it may have
been robbed by the extra track.

Code 2 is essentially the same as Code 1 except that the extra
track interacts in one of the large chambers. Also those cases where
the extra track was an electron were given a code of 2.

Codes 3, 4, and 7 are self-explanatory. Code 5 refers to those
cases where a beam track interacted before it reached the target and
Code 6 to those cases where it interacted after it left the target.
Code 8 was used when a neutron interacted in one of the large chambers
producing either a proton recoil or a neutron star. The tracks in
both cases were short and heavy and very straight in comparison with
those made by gamma rays. Also the proton recoils usually did not
point to the target. Code 9 was given to events which did not fit
into any of the other categories and for which an unambiguous explana-
tion of the event was impossible.

Neutron Detector Codes

0 --- Good recoil track

1 --- Gamma ray converted in neutron detector

2 --- A recoil has no visible sparks in at least one view

3 --- Two or more adjacent neutron detector lights off between the first and last light of the track

4 --- One light on in front of a good recoil track

5 --- The track begins more than two spark chambers in front of the first light that is lit

6 --- Good recoil track with a reflection

7 --- Multiple tracks where both tracks are in the region where the lights are on

8 --- Multiple tracks where only one track is in the region where the lights are on

9 --- Charged particle entered neutron detector

Most of these codes are self-explanatory except for Code 6 and Code 9. Code 6 refers to the case where reflections off the spark chamber faces produce what appears to be a second spark parallel to but fainter than the actual spark. Code 9 was used to identify those portions of film where we allowed elastically scattered pions to enter the neutron detector in order to calibrate the timing of the pairs of counters in the detector.

After the event had been assigned an event code, the large chambers were checked to see if they contained any gamma rays. If they did the gammas were categorized as being either a certain, short, or doubtful gamma. A certain gamma was one which points well to the target and has either four sparks in seven gaps, or five sparks in nine gaps, or more than five sparks. Certain gammas which clearly did not point

to the target were flagged in the geometry program and were not

considered as part of the event. Short gammas were those with three

sparks in consecutive gaps which seemed to point to the target and

did not have the characteristics of a recoil proton. Doubtful

gammas were those which did not satisfy the gap criteria of did not

point to the target well or pointed to the target but had the appear-

ance of a neutron recoil.

Two rolls of film were rescanned by the scanners as a check on

scanning efficiency and the results of the initial and final scans

were examined by a physicist. It was found that approximately 7%

of the events had a change in classification and that these changes

were rather minor usually resulting from differences of opinion as

to the quality rather than the type of event. These changes in

classification were found to be uncorrelated with event type and

to make no difference in the ratio of measured to unmeasured events

in the sample.

Measuring

In order to minimize the chance of misinterpretation only those events which had a main array code of 0, 1, or 2 and a neutron detector code of 0, 6, or 8 were measured. This meant that the person doing the measuring had to deal with at most two beam tracks one of which passed straight through the target. Such events were found to present no problems in interpretation; however, if more than one extra beam track was present, the chances of making a mistake in identifying the beam track which caused the interaction were greatly increased. Also the presence of several extra beam tracks in the downstream large chamber increased the chance that any gammas which were present in that chamber would be seriously robbed. The acceptable codes in the neutron detector were chosen so that it was possible to uniquely identify the track responsible for the timing signal and to be reasonably certain that the neutron did not scatter in the detector before converting or that the recoil track did not enter the detector from outside the fiducial volume.

For those events which did not have an acceptable event code only one card, called a head card, was prepared. The head card contained such information as the roll and frame number, the event code, the number of gammas in each category in the event, and several codes which were used for bookkeeping purposes.

The measuring was done using image plane digitizers (IPD). The IPD used a Prevost projector to project a magnified image of the film

onto a flat surface. The coordinates of each measured point on the surface were encoded in arbitrary units (10,000 along each axis) and were punched on an IBM card.

To check the measuring accuracy the scanners measured points on a precision grid. It was found that the spread in these measurements was approximately three table units or roughly 1 mm. in space. This was certainly adequate for our purpose since the overall error on the determination of the geometry parameters used in the reconstruction of the events in space was found to be about 2 1/2 mm. in space.

In each picture as many beam points as possible up to a maximum of six were measured. In the maximum case there were two points in the large chamber and four points in the small chamber. Next the conversion point of each gamma ray in the picture was measured. Finally an even number of points along the recoil track in the neutron detector were measured with two of the points being the first and last points on the track. The term 'measuring' as used here means that a measurement of each point was made in both the direct and the side view.

Also one point was measured on each A-D light and each neutron detector light which was lit. These points were used by the geometry program to determine the neutron time-of-flight as seen by the A-D circuitry and which neutron detector counters gave signals for that event.

Data Handling Programs

All the programs which were used in this experiment were run on an IBM 360/65 computer. The geometry program which was called GEOSPK had as its input the IBM cards from the IPD's. The program performed the spatial reconstruction of the measured events and also printed a list of those events for which it was unable to complete the reconstruction. The list contained the roll and frame number of the event and the reason why the event failed. The failing events were remeasured and then reprocessed by the geometry program. The output from the geometry program was a binary tape containing the geometrical information for each measured event and the information on the head card for each unmeasured event. For a more complete description of the geometry program see Appendix C .

The output tape from the geometry program was used as input to a program called SCANTY. This program added kinematical information to the geometrical information already present for each event. The program also determined which counter pair in the neutron detector gave the timing signal and checked that the recoil track in the neutron detector was within the fiducial volume.

During the run data was taken at six different beam energies. The roll and frame number at the beginning and end of each energy region were used to establish the correspondence between roll and frame number and beam energy. This correspondence was read into SCANTY as a table. It was then possible to determine the central

value of the beam energy for a given event by using the roll and
frame number for that event and doing a table lookup.

To find the energy of the neutron it was necessary to do several
preliminary calculations. First the time-of-flight of the neutron
was calculated from the A-D value. Next the beta of the neutron was
calculated from the time-of-flight and the distance to the counter pair
which gave the timing signal. Finally the energy of the neutron
was computed using its mass and beta.

The next step was to calculate the missing mass for each event.
Since it now knew the angle of the neutron with respect to the beam
and the neutron's energy, SCANTY made the calculation using the formula:

$$(E_T - E_N)^2 - (\vec{P}_B - \vec{P}_N)^2 = M^2$$

(1)

where E_T is the sum of the incident beam energy and the mass of a proton,
E_N is the neutron energy, $\vec{P}_B$ is the beam momentum, $\vec{P}_N$ is the neutron
momentum, and M is the missing mass.

As its output SCANTY wrote a binary tape containing the geometry
information and the missing mass, beam energy, and neutron energy for
each event. The assignment of energies to the gamma rays in the event
was not done by SCANTY. The output tape had the value zero for each
gamma energy.

The assignment of gamma ray energies was done using a procedure
known as spark counting which is described in Refs. 21 and 22 . It

consisted of counting the total number of sparks associated with the shower created by the conversion of a gamma ray in the large chambers. The energy of the gamma in MeV was then given by the formula:

$$E = (6.1 \, N + 16.1)/A \qquad\qquad (2)$$

where N is the number of sparks in the shower and A is the cosine of the angle between the gamma direction and the normal to whichever chamber the gamma converted in. Formula (2) was determined in the following fashion: first the two gamma events were processed by a kinematical fitting program called FITSPK which is described later in this section. Next a sample of two gamma events which were fit successfully either as an eta or a pi zero event was selected. A correlation between the number of sparks visible in the shower and the corrected gamma energy was plotted for the selected sample. The corrected energy was the value of the fitted energy times the cosine of the angle between the gamma direction and the chamber normal as described above. Formula (2) is the result of fitting a straight line to the plotted points. For more detail on the determination of formula (2) see Ref. 20.

The gamma energies given by formula (2) were not very precise. The errors on these energies were large, varying from roughly 20% for gammas of about 400 MeV and 50% for gammas around 100 MeV to 100% for gammas near 40 MeV. These errors reflected the lack of knowledge as to how much of the total energy of the gamma ray was actually visible

in the shower. A number of effects such as mild robbing or obscuring

of individual sparks contributed to this lack of knowledge. Those

events where a gamma was severely robbed or left the chamber were

excluded from the straight line fit.

Although the energies determined in this fashion were imprecise,

they did represent an estimate of the minimum energy physically possible

for each gamma ray. Such energies, particularly in the case of three

or more gamma events, were very useful as initial values of the gamma

energies for the kinematical fitting program. The two gamma events

were less complex and so the spark count energies were of less use

in fitting those events.

The kinematical fitting program mentioned earlier was called

FITSPK. It used the output tape from SCANTY either with or without

spark count energies as its input. The program, using the energies

and direction cosines from SCANTY, attempted to fit each event to

one of the hypotheses available for that type of event. For example,

in the case of a four gamma event the program would attempt to fit

the event to either two pi zero production or eta production with the

eta decaying to a pi zero and two gammas. The results of each fit

were printed and were also written on a binary output tape.

Results
_____

The results presented in this section are based on the analysis

of the data contained in 17 2/3 rolls of film. The rolls were 1000

feet in length and there were approximately 3000 pictures on a roll.

Most of the rolls (13 1/3) were taken with an incident beam momentum

of 752.5 MeV/c. Also there was 2/3 of a roll taken at 769.5 MeV/c,

1 roll at 744.5 MeV/c, and 2 2/3 rolls at 721.5 MeV/c. The 2 2/3

rolls at 721.5 MeV/c were used to determine the background in our sample

since for that value of the beam momentum it was kinematically

impossible for the reaction $\pi^- + p \rightarrow \eta^0 + n$ to produce neutrons in

the angular region covered by the neutron detector.

It was assumed that the background was produced by the following

reactions

$$\pi^- + p \rightarrow \begin{cases} \pi^0 + n \\ 2\pi^0 + n \\ 3\pi^0 + n \end{cases}$$
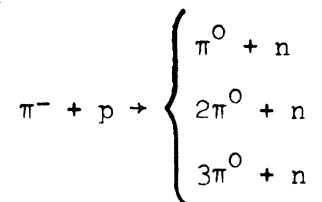
Assuming a phase space model for the $2\pi^0$ and $3\pi^0$ reactions the proba-

bility for observing their partial decay modes in our chambers has been

determined with a Monte Carlo program called NVERTX (see Appendix D).

A fit to the number of $2\pi^0$ and $3\pi^0$ parents in the background was made

using the NVERTX probabilities and the number of three, four, and six

gamma events (there were no five gamma events seen in the background).

The fit gave the number of $2\pi^0$ parents as 64 ± 21 and the number of

parents as -2 ± 14 with a chi square of 1.57 for one degree of freedom.

The fit was consistent with there being no $3\pi^O$ background in the 721.5 MeV/c data.

NVERTX was used to generate the detection efficiency of the neutron detector and the probability of seeing the various partial modes for the $3\pi^O$ reaction at beam momenta of 721.5 MeV/c and 752.5 MeV/c. Both the detection efficiency and the probabilities for the partial modes were the same within less than one standard deviation at the two momenta. This means that the absolute probability of detecting a $3\pi^O$ background event was the same within one standard deviation for the 752.5 MeV/c data as for the 721.5 MeV/c data. When this process was repeated for the $2\pi^O$ reaction, the same conclusion was reached. Since the cross sections for $2\pi^O$ and $3\pi^O$ production did not change appreciably over the region of momenta with which we were concerned (see Ref. 23), we concluded that the data at 721.5 MeV/c should give a good representation of the background in the 752.5 MeV/c data.

To compute the $2\pi^O$ and $3\pi^O$ background in the 752.5 MeV/c data it was necessary to scale up the 721.5 MeV/c data until the number of incident beam pions was the same for both samples. The appropriate scale factor was found to be 5.23. Since the 721.5 VeV/c data was consistent with having no $3\pi^O$ background, we assumed that there was no $3\pi^O$ background in the 752.5 MeV/c data. Using the results of the fit for the 721.5 MeV/c data and the scale factor the predicted number of parent $2\pi^O$ background events in the 752.5 MeV/c data was 336 ± 107.

For the moment we ignored the possible presence of $a\pi^0\gamma\gamma$ decay mode of the eta. We made a model for the production of events with more than two gammas assuming that there existed six gamma parents from $\eta^0 \to 3\pi^0 \to 6\gamma$ and four gamma parents from $2\pi^0 \to 4\gamma$. NVERTX was used to generate the probabilities for seeing the partial modes of these two parents. We then fit the three, four, five, and six gamma events in the 752.5 MeV/c data to our model. The fit gave the number of $2\pi^0$ parents as 243 ± 49 and the number of $3\pi^0$ parents as 214 ± 28 with a chi square of 0.69 for two degrees of freedom. The fitted number of $2\pi^0$ parents was within one standard deviation of the number predicted from the 721.5 MeV/c data. We concluded that the events with more than two gammas were completely explained as being the result of $2\pi^0$ and $\eta^0 \to 3\pi^0$ decays and did not require the presence of an $\eta^0 \to \pi^0\gamma\gamma$ decay mode.

In order to establish a limit for the number of $\pi^0\gamma\gamma$ parents which could exist in our data we removed the events which have $2\pi^0$ and $3\pi^0$ parents from the three and four gamma events and used the remaining number of events to compute the number of $\pi^0\gamma\gamma$ parents. The number of $3\pi^0$ parents which appeared as three and four gamma events was calculated by multiplying the fitted number of $3\pi^0$ parents by the NVERTX probability for seeing $3\pi^0$ parents as three and four gamma events respectively. The process was repeated for the $2\pi^0$ parents except in that case the number predicted from the 721.5 MeV/c data was used for the number of $2\pi^0$ parents. After performing the subtraction

there were -25 ± 30 three gamma events and $^-9 \pm 16$ four gamma events. Using these numbers and the NVERTX probabilities for seeing $\pi^0\gamma\gamma$ parents in our data was $^-68 \pm 69$. Based on this result we assumed that there were no $\pi^0\gamma\gamma$ parents in our data.

To determine the number of $\eta^0 \rightarrow 2\gamma$ parents we had to remove from the two gamma events both the falldown from $2\pi^0$ and $3\pi^0$ parents and the events from $1\pi^0$ parents. A convenient technique for eliminating the $1\pi^0$ events was to make a cut on the opening angle of the two gammas in the π^-p center of mass (see Ref. 5). At a beam momentum of 752.5 MeV/c the minimum center of mass (CM) opening angle for two gammas from $1\pi^0$ parents was 33^0 while the minimum CM opening angle for two gammas from etas was 146^0. The CM opening angle distribution for $1\pi^0$ events was such that a negligible number of the events had gammas with opening angles greater than 100^0. There were, therefore, no $1\pi^0$ events in the eta region which had opening angles from 140^0 to 180^0. The CM opening angle distribution for the 2γ events in the 752.5 MeV/c data is shown in Fig. 5. Since we did not have perfect resolution, the peaks from the π^0 and the η^0 occur at 30^0 and 140^0 respectively. The remainder of the events were falldown from $2\pi^0$ and $3\pi^0$ parents.

Events where an eta was produced had a neutron beta spectrum which ranged from 0.26 to 0.65. In addition, for etas which decayed into two gammas the CM opening angle of the two gammas would be greater that 140^0. To determine the number of two gamma events from eta parents

we established the criterion that we would consider only those events which had a neutron beta between 0.26 and 0.65 and a two gamma CM opening angle greater than 140°. From a plot of neutron beta versus the CM opening angle for the two gamma events in the 752.5 MeV/c data (see Fig. 6) we found that there were 152 events which satisfied our criterion. From these events we had to eliminate the falldown from $2\pi^\circ$ and $3\pi^\circ$ parents. Using NVERTX we could generate two gamma events which came from $2\pi^\circ$ and $3\pi^\circ$ parents and then plot the neutron beta versus the CM opening angle for these events. From these plots we could determine the probability that a two gamma event from either $2\pi^\circ$ or $3\pi^\circ$ parents would satisfy the above criterion for being a two gamma event from an eta. For two gamma events from $2\pi^\circ$ parents this probability was 0.143 ± 0.014 and for two gamma events from $3\pi^\circ$ parents the probability was 0.075 ± 0.020. Using these probabilities along with the NVERTX probabilities we could compute from the fitted numbers of $2\pi^\circ$ and $3\pi^\circ$ parents how many two gamma events from $2\pi^\circ$ and $3\pi^\circ$ parents would appear as falldown in the 152 two gamma events in the 752.5 MeV/c data. This number was found to be 10 ± 2 events. Subtracting this number from the 152 two gamma events and then using the NVERTX probability we obtained 302 ± 27 as the number of parent etas which decayed into two gammas.

It should be noted that the number of parent two gamma etas was insensitive to the presence of a $\pi^\circ\gamma\gamma$ decay mode of the eta. The probability for seeing two gammas from either $2\pi^\circ$ or $\pi^\circ\gamma\gamma$ parents

was the same within one standard deviation and the CM opening angle distribution for two gammas from $2\pi^0$ or $\pi^0\gamma\gamma$ parents was also very similar. The amount of falldown in the two gamma events would, therefore, be the same whether it came from $2\pi^0$ parents or from $\pi^0\gamma\gamma$ parents. Since the majority of the total falldown in the two gamma events came from four gamma parents, the amount of falldown to be subtracted from the two gamma events would not change if there should be $\pi^0\gamma\gamma$ parents present in the data. So the number of parent etas which decayed into two gammas would be unaffected by the presence of a $\pi^0\gamma\gamma$ decay mode of the eta.

The ratio of the number of etas which decay into two gammas to the number of etas which decay into $3\pi^0$ is

$$R(2\gamma/3\pi^0) = 1.41 \pm 0.22$$

Using the number of $\pi^0\gamma\gamma$ parents presented earlier in this section the ratio of $\eta^0 \rightarrow \pi^0\gamma\gamma$ to the sum of $\eta^0 \rightarrow 2\gamma$ and $\eta^0 \rightarrow 3\pi^0$ is

$$R(\pi^0\gamma\gamma/2\gamma + 3\pi^0) = -0.13 \pm 0.13$$

Based on the above result we could say that the decay mode $\eta^0 \rightarrow \pi^0\gamma\gamma$ was equal to no more than 9% of the sum of the decay modes $\eta^0 \rightarrow 2\gamma$ and $\eta^0 \rightarrow 3\pi^0$ with a confidence level of 90%. The ratio of $\eta^0 \rightarrow 2\gamma$ to the sum of $\eta^0 \rightarrow 2\gamma$ and $\eta^0 \rightarrow 3\pi^0$ is

$$R(2\gamma/2\gamma + 3\pi^0) = 0.59 \pm 0.07$$

The ratio of $\eta^0 \rightarrow 3\pi^0$ to the sum of $\eta^0 \rightarrow 2\gamma$ and $\eta^0 \rightarrow 3\pi^0$ is

$$R(3\pi^0/2\gamma + 3\pi^0) = 0.41 \pm 0.06$$

So far little has been said about the use of the kinematic fitting

program called FITSPK. Both the two and four gamma events were pro-
cessed by FITSPK. An attempt was made to fit the four gamma events
as coming from either $2\pi^0$ production or the $\pi^0\gamma\gamma$ decay of an eta. Very
few events fit successfully and almost none of those which fit gave
unambiguous results. In order to determine whether FITSPK or the data
was at fault NVERTX was used to generate $2\pi^0$ events and these events
were put through FITSPK. Although the success rate was somewhat
higher for these events, the fits still gave ambiguous results. At
this point it became clear that FITSPK lacked the sophistication necessary
to analyze properly the three, four, five, and six gamma events.

In the case of the two gamma events the situation was considerably
improved. When NVERTX two gamma eta events were put through FITSPK,
the program found the right solution in almost every case. However,
the chi square distribution for the two gamma events in the data which
fit successfully to an eta was somewhat broader than a similar distri-
bution for the fits of NVERTX generated two gamma eta events. Since
the two gamma events could be readily analyzed by other techniques,
there seemed to be no point in complicating the analysis by the use
of the fitting program.

Although it was not used in the analysis, FITSPK was used to
determine the range of neutron betas which were measured by the A-D
circuitry for the two gamma eta events. Also it was through the
study of the unsuccessful two gamma fits that we discovered the necessity
of eliminating those events where a gamma converted within 4 cm. of

the neutron detector hole in the downstream large chamber. This

is discussed further in Appendix D .

CONCLUSIONS

The results of this experiment are in good agreement with the fitted results of the new experiments quoted earlier in this thesis. The agreement with the fitted results of the old experiments is not as good. The following table gives a comparison of the branching ratios obtained from the various experiments.

	$R(2\gamma/3\pi^0)$	$R(\pi^0\gamma\gamma/2\gamma + 3\pi^0)$
This experiment	1.41 ± 0.22	-0.13 ± 0.13
New experiments	1.503 ± 0.208	0.014 ± 0.024
Old experiments	1.886 ± 0.362	0.366 ± 0.067

Our results for the 2γ to $3\pi^0$ branching ratio are consistent with both the new and the old experiments. The branching ratio which we obtained for $\pi^0\gamma\gamma$ to $2\gamma + 3\pi^0$ is consistent with the new experiments but not with the old experiments. Both our results and the results of the new experiments indicate that the $\pi^0\gamma\gamma$ decay of the eta is at most a small fraction of the total neutral decays. If these results are correct, then the existence of the A quantum number suggested by Bronzan and Low (7) would seem to be in doubt unless some reason can be found for the suppression of the $\pi^0\gamma\gamma$ mode with respect to the other neutral decay modes.

Our results are consistent with the branching ratios predicted

by Chan (8) using a model based on Schwinger's field theory of matter. His predicted ratios are 1.07 for $2\gamma/3\pi^0$ and 0.04 for $\pi^0\gamma\gamma/2\gamma + 3\pi^0$.

The ratio of $\pi^0\gamma\gamma$ to 2γ decays in our data is -0.225 ± 0.229. This is consistent with a prediction based on a quark model by Van Royen and Weisskopf (18). Their prediction for $\pi^0\gamma\gamma/2\gamma$ is 0.0005.

Appendix A

The electronic logic received as input pulses from scintillation counters in the beam telescope, the neutron detector, and from several anti-counters. The pulses were the output of Amperex 56 AVP phototubes. For the counters in the beam telescope and neutron detector the dynode pulse was delayed by one nanosecond and then mixed with the anode pulse to give a sharp, narrow pulse.

A diagram of the electronic logic is given in Fig. 7 . The logic was composed of Chronetics Nanologic modules except for the A-D circuitry and the circuitry for lighting the electroluminescent panels on the neutron detector which were built from DEC flip-chip modules.

An event resulted from a coincidence of the beam telescope, given by $123\bar{3}'\bar{4}\bar{4}'$, and a pulse from the final neutron detector fan-in and the anti-coincidence of the neutron detector anti-counters. In order to make coincidence the beam telescope pulse was stretched to cover the range of time in which a pulse from the neutron detector might arrive. This "time window" for event coincidence was set at 48 nanoseconds. The leading edge of this window was set by varying delay D3 with respect to D2. In this way it was possible to select a range in time-of-flight which eliminated gamma rays and most of the fast charge exchange neutrons from our data.

The timing for the neutron time-of-flight was done by measuring the overlap of a pulse from the neutron detector with a reference pulse from counter 1. The pulse from counter 1 was gated by the require-

ment that it be in coincidence with both the beam telescope and the event coincidence to prevent extraneous pulses due to the high beam flux from overloading the discriminator of counter 1 and passing through to the time-to-pulse-height converter. Both the beam telescope and the event coincidence pulses were stretched to cover the range of pulses coming from counter 1. The pulse from counter 1 was kept narrow so that it was the pulse which gave the coincidence in each case. After the coincidence gates the pulse from counter 1 was shaped and stretched to cover the range of pulses from the neutron detector and then fed into the time-to-pulse-height converter. The neutron detector pulse was also shaped before being put into the converter. The maximum possible overlap of the two pulses was controlled by varying delay D1 with respect to D4. These delays were set so that faster times-of-flight gave more overlap and so that the pulse from the neutron detector could not arrive at the time-to-pulse-height converter before the reference pulse even for the fastest possible time-of-flight. This prevented foldover in the A-D values.

The logic was made ready to detect events by receiving a signal which was synchronized to the Cosmotron beam spill. This signal turned off a gate which was normally on and which prevented the beam telescope and neutron detector from accepting events. Whenever an event was detected, a signal was sent which turned the gate back on. This prevented the logic from detecting another event before the first event had been completed. It also prevented the logic from picking

up Rf noise when the spark chambers fired. If no event was detected, the gate was reset internally after a set time which depended on the length and quality of the beam spill. The gate was turned off during the middle of the spill to avoid the beam spikes at the front and back of the spill.

After an event had been detected, a signal was sent to a power fan-out which gave out two signals. One was used to trigger the spark chambers and the other provided the gate signal for the electrolumin-escent panels on the neutron detector. The DEC circuitry lit a panel whenever a pulse from the appropriate counter's discriminator was re-ceived by the circuitry in coincidence with the gate pulse.

The relationship of the functions performed by the slow logic after detection of an event is shown in Fig. 8 .

Several of the counters shown in Fig. 7 have not been described so far. These are the two beam monitors and the up and down counters. The beam monitors were placed near the beam transport system and were subject to such high fluxes of particles that they gave unreliable re-sults and so were not used. The up and down counters were placed above and below the target respectively. Their purpose was to detect charged particles which went out of the top or bottom of the array and were not seen in the small chambers. However, their relatively low efficiencies made them of limited usefulness.

Appendix B

To calculate the neutron time-of-flight it was necessary to convert the value of the A-D lights from channel number into seconds. The conversion factor from channel number to time was determined using the following technique. The output from a pulse generator was divided into two signals. One signal was fed directly into the time-to-pulse-height converter. The other signal was given a fixed delay before being fed into the converter. Initially the value of the delay was set at zero which determined the channel number for the maximum overlap of the two pulses. The delay was then increased and a new value of the channel number was obtained. By repeating this process with a slightly different delay each time it was possible to correlate channel number with a given delay between the two signals.

In our case we varied the delay from 0 to 41 nanoseconds in steps of 1/2 nanosecond. The resulting curve of channel number versus time was found to be reasonably linear except for very low channel numbers. This curve was called the calibration curve.

During the run two points on the linear portion of the curve were taken usually twice for each roll of film. SCANTY shifted the calibration curve to pass through the two points and used the resulting curve to convert from channel number to time.

The time-of-flight of a neutron to its interaction point in the neutron detector is related to the A-D time by the following equation:

$$T_{AD} = T_N + T_R + T_V + T_O \tag{4}$$

where T_{AD} is the A-D time, T_N is the neutron time-of-flight, T_R is the time taken for the proton recoil to travel from the inter-action point to the center of the counter pair giving the signal, T_V is the time required for the light to travel through the scintillator to the phototube, and T_0 is a constant time for each counter pair which relates the relative time between pulses as measured by the electronic circuitry to the actual time-of-flight taking into account the delays introduced by the phototubes and bases, the cables connecting the various parts of the equipment, and the logic itself.

Although the proton recoil created by a neutron might have travelled through several counter pairs, it was possible to determine which pair gave the timing signal. The first signal coming from the neutron detector was used for the timing so if several counter pairs gave signals the one with the smallest value of T_{AD} gave the timing. Since for a given neutron T_N was a constant, T_{AD} would have its smallest value when the sum of T_R, T_V, and T_0 had its smallest value. So the counter pair giving the timing signal was the pair which had the minimum sum of T_R, T_V, and T_0 of all the pairs which gave signals.

To calculate T_R for each counter pair which gave a signal SCANTY used the range remaining in the recoil track as an estimate of the energy of the recoil at a given point. From this it could calculate the velocity of the recoil at any point. It then computed T_R as the time required for the recoil to travel from the interaction

point to the middle of a given counter pair. The middle of
the counter pair was used since the delays associated with the in-
dividual neutron detector counters were such that it was not known
which of the two counters in a pair was responsible for the coinci-
dence signal. This ambiguity as to which counter caused the signal
resulted in an uncertainty in T_R of no more than 0.5 nanoseconds
for any counter pair.

The time T_V was calculated by computing the distance from the
recoil track in the counter to the phototube at the top of the
counter and dividing this distance by the speed of light in the
counter. To calculate the speed of light in the counter the effec-
tive index of refraction of the counters as measured in Ref. (24)
was used. The distance to the top of the counter was taken as the
average of the distances in the two counters for the reason previously
stated.

The constant T_0 was obtained for each counter pair separately.
The anti-counters in the front of the neutron detector were removed
from the logic so that elastically scattered pi's and protons could
pass through the detector. The voltage was removed from all but one
pair of counters. For each counter pair several hundred pictures
were taken in this configutation. The pictures were scanned for
the distinctive signature of a π - p elastic scattering with both
tracks visible in the chambers. Events where the pion went into the
neutron detector looked quite different from events where the proton

went into the neutron detector. This allowed the unambiguous identification of the particle in the neutron detector.

Those events which had a good, clear signature and where the particle going into the neutron detector did not scatter in the large chambers were measured and sent through the geometry program. From the geometry information and the known beam energy it was possible to determine the velocity of the particle going into the neutron detector. The velocity of the protons was corrected for the energy lost in the counters as they passed through the neutron detector. Such a correction was negligible for pions. The time-of-flight was calculated using the velocity of the particle and the distance from the target to the middle of the chosen counter pair. Using this value as T_N and from the known value of T_{AD} and computed value of T_V (T_R is zero in this case) equation (4) could be solved for T_0 for a given counter pair. The process was repeated until a solution for T_0 was obtained for all counter pairs.

The distribution of values of T_0 for a given counter pair was found to have a standard deviation of approximately two nanoseconds. This was much wider than was expected on the basis of the electronic resolving times. This effect was not completely understood but it was suspected that RF pickup might have been creating noise in the A-D circuitry and that this noise was responsible for the width of the observed distribution.

Appendix C

The geometrical reconstruction program was called GEOSPK. It was specifically designed to handle events which contained charged tracks and gamma rays in the same picture. The input was in the form of punched cards containing identification and coded information for each event along with the coordinate points from the IPD's for each track. The output consisted of a binary tape with identification and geometrical information for each event plus a printed list of those events which failed one or more of the geometry tests.

The program began by reading in a number of parameters such as the system transformations mentioned earlier. It then read in the data cards one event at a time and determined whether or not the event had measurement cards associated with it. If not, the program wrote an identifying record on the output tape and proceded to the next event. If there were data cards for that event, the program checked to make sure the fiducials were measured properly by transforming into a known system using three of the four fiducials and then checking that the fourth fiducial was within set limits from its proper position. The program then used the four fiducials to set up a transformation to the normalized film plane. This was a homographic transformation which standardized the coordinate systems of the several IPD's and also served to remove any linear distortions caused by the projection system. This transformation was applied to all coordinate points as they were read in and stored.

Next the value of the binary lights recorded on the film was
determined. These lights represented the neutron time-of-flight
as measured by the analog to digital circuitry. One point as close
to the center as possible was measured for each light that was on.
The program knew the outer limits of the region for each light in
the standard coordinate system and so by determining in which
region the measured points lay it could decide which lights were on.
It then added together the values of the lights to arrive at the
final value.

After this the coordinate points associated with the two views
of each track were read into a track bank. A track in this case
means one particular object such as the beam or a gamma ray, or a
charged particle. The number of measured points associated with each
track was usually very different so the program kept track of how
many points were associated with each track. It also checked to make
sure that the number of points measured in the direct and side views
of each track were the same. The tracks were assigned numbers which
served to identify them as to the particle which they represented
and whether the track was from the direct or side view.

When all the tracks belonging to one event had been read in, the
geometrical reconstruction began. The points on each track were recon-
structed in space by transforming the points in the direct and side
views to their respective chamber faces and then, knowing the camera
positions in each view, projecting a line from the camera through each

point into the chamber. The intersection of the lines projected
through the direct and side views gave the location of the original
spark in the space of the chamber (see Fig. 4). The points in the
space of the chamber were then transformed into the main coordinate
system and stored in another track bank.

The program checked the beam track to make certain that two or
more points were measured. If only two points were measured, those
two points were used to determine the beam line. If three or more
points were measured, an attempt was made to fit a straight line to
the beam track. If the fit produced a chi square which was larger
than a set limit and there were more than three points on the track,
then the point with the largest error was eliminated and the fit
was retried. If this fit failed or there were only three points on
the track for the first fit, the beam line was determined by the two
points with the greatest separation.

The program next checked to see if the event contained any charged
prongs. If so the program attempted to fit a straight line to each
charged prong provided there were three or more points associated with
that track. If the fit failed, the program proceeded as in the case of
the beam track. When there were two points on the track, the program
used them to determine the direction of the track. If there was only
one point on the track, the program stored the track number so that
after the interaction point had been determined it could construct
the track's direction from the interaction point and the one point of

the track.

If the program could determine the direction of one or more charged prongs, it tried to do a fit for the interaction point. For the fit it used the two points with the greatest separation on each track. If a straight line had been successfully fitted to the track, it used the fitted values of the two points with the greatest separation. It then fitted for the intersection of the beam track and the charged prongs. When the program dealt with neutral events, or if there were not enough charged prongs to fit for the interaction point, the program projected the beam track to the center plane of the target and took the intersection of this plane and the beam track as the interaction point. In either case it checked the resulting interaction point to make sure that it was inside the limits of the target. It also checked that the errors on the determination of the interaction point were within set limits. Finally it computed the direction cosines for each track using the interaction point and the point on the track which was farthest away from the interaction point.

For charged prongs the program checked to see whether or not there were range points in the large chambers. If there were, it stored the number of such points, the points, and the number of the chamber in which the point was located. It also stored a code which told whether or not the track left the chamber.

Next the program processed the information from the neutron detector. It found out which lights were turned on and how many lights

were on. It checked that the number of lights which were on was less than or equal to a set limit. It also checked that an even number of points had been measured.

To determine the neutron's conversion point the program used the first two measured points in the neutron detector to form a line and projected that line to the center plane of the preceding scintillation counter. The intersection of the line and the plane was called the neutron conversion point. The program used this point and the interaction point to compute the direction cosines of the neutron.

Finally the program wrote the information it had obtained for the event onto an output tape. The first five words of this tape contained the roll and frame number, the date of measurement, the event code, and various flags in packed format. The rest of the information consisted of the interaction point and its errors, the chi square of the fit for the interaction point if such a fit existed, the direction cosines with errors for all particles in the event, range points for the charged prongs, and the points in the neutron detector including the conversion point.

Appendix D

A general Monte Carlo program called NVERTX (see Ref.25) was
used to determine the probability of detecting a particular type
of event in our experimental apparatus. The program generated
events using n-body phase space and a rejection technique to determine
the energy and direction cosines of the particles in the event. This
information was passed to an experimental function which determined
whether or not that event would be detected by the experimental
apparatus. NVERTX can also display the distributions of various
quantities such as the energy or production angle for a particle
or series of particles.

In order for NVERTX to give meaningful results the experimental
function must duplicate as closely as possible the geometrical setup
of the experimental apparatus. NVERTX provides a one hundred location
parameter bank which was read in at execution time for this purpose.
The experimenter can use as many of the parameters as necessary to
provide the experimental function with an accurate picture of his
experimental setup.

After receiving the energy and direction of each particle in
an event, the experimental function determined an origin for that
event. The coordinates of the origin were chosen so as to be randomly
distributed throughout the inside of the hydrogen target. The z
coordinate was then shifted to the center plane of the target since
for neutral events in the data the z coordinate of the origin was

taken at the center plane of the target.

It is possible to have NVERTX pass to the experimental function only those events which have the production angle of the neutron in the angular region covered by the neutron detector. The experimental function divided the azimuth into thirteen angular regions. The entire event was rotated so that the azimuthal angle of the neutron fell in the angular region covered by the neutron detector. These two steps resulted in a considerable increase in the efficiency of the program and shortened the time necessary to generate a given number of events.

To determine whether or not the neutron interacted in the neutron detector the experimental function used the equation

$$PROB = 1 - \exp(-X/\lambda(P)) \tag{5}$$

where PROB is the probability of interaction, X is the distance travelled in scintillator and $\lambda(P)$ is a momentum dependent mean free path. The experimental function threw a random number between zero and one which it used for the probability in equation (5). It then solved for the distance X and compared this distance to the potential path of the neutron through the scintillators in the neutron detector. If the distance was less than the potential path, it said that the neutron interacted. If not it said that the neutron was not seen and went to the next event. No attempt was made to correct for the cases where the proton did not leave the scintillator or did not reach the next scintillator before it left the neutron detector.

If the neutron interacted in the neutron detector, the experimental function calculated the coordinates of the interaction point and then spread them according to a Gaussian distribution with a width corresponding to the measuring error on points in the neutron detector. It then used the interaction point and the origin to calculate new direction cosines for the neutron. It also calculated the time-of-flight of the neutron and gave this time a Gaussian spread with a width of two nanoseconds corresponding to the spread in the constant calibration time for each counter pair (see Appendix B).

The program handled the conversion of gamma rays in the large chambers in a similar fashion. In this case the equation used is

$$PROB = 1 - \exp{(-X/\mu(E))} \qquad\qquad (6)$$

where PROB and X are the same as for equation (5) and

$$\mu(E) = X_o/C(E)$$

where X_o is the radiation length and is equal to 1.8 cm. for iron and 41.3 cm. for scintillator and

$$C(E) = -0.42 + 0.309 \log{(E)} - 0.02(\log{(E)})^2$$

where E is the laboratory energy of the gamma ray. The program proceeded as in the neutron case and solved for the conversion distance of the gamma ray. If this distance was less than the potential path of the gamma ray through the large chamber and if the energy of the gamma ray normal to the chamber face was greater than the low energy cutoff, then the program said the gamma converted and was seen, The program kept track of how many gammas from a given event were seen.

If a gamma ray converted in an anti-counter or in the neutron detector, a flag was set and that event was discarded.

The low energy cutoff was the minimum energy necessary to create three sparks in a large chamber. Since we did not accept gammas with less than three sparks in the data, we needed to know how much energy these three-spark gammas have so that NVERTX could classify gammas with less than that energy as being unseen gammas. The events containing three or more gammas were quite sensitive to the low energy cutoff. We assumed that there existed four gamma parents and six gamma parents and that both parents were produced according to phase space. We then used NVERTX to generate the probability of seeing the fractional modes of each parent with different low energy cutoffs spaced 10 MeV apart from 20 MeV to 60 MeV. Using these sets of probabilities we fit the three, four, five, and six gamma events for four and six gamma parents. The fit using the set of probabilities with the proper low energy cutoff should have the best chi square. A plot of the chi square versus the low energy cutoff is shown in Fig. 9. Based on this plot we chose 34 MeV as being the best value of the low energy cutoff for our chambers.

It was discovered upon examining the two gamma events which did not fit successfully to either an eta or pi zero that many of these events had neutron betas greater than 0.8. It was also observed that most of these events had a gamma ray which converted near the hole in the downstream large chamber. These events were assumed to be the re-

sult of a soft gamma, produced in the shower from the original gamma, converting in the neutron detector. This gamma was responsible for triggering the neutron detector instead of a neutron. This assumption was checked by plotting the neutron beta spectrum of those events which had gammas converting outside of a square region of varying size around the neutron detector hole. It was found that by rejecting events where a gamma ray converted within a 4 cm. square around the neutron detector hole 70% of those events with a neutron beta greater than or equal to 0.8 were eliminated whereas 49% of the events with a neutron beta less than 0.8 were eliminated. (See Figs. 10 and 11). The events in the eta region of the spectrum ($\beta < 0.65$) were decreased by 45%. Based on this result a cut which eliminated from the sample those events where a gamma ray converted within 4 cm. of the neutron detector hole was applied to the data. The same cut was added to the experimental function so that NVERTX generated events would satisfy the same criteria as the data.

NVERTX was used to generate the probability for seeing a given number of gamma rays both from the various eta neutral decay modes and from the background neutral decay modes. The resulting probabilities are given in Table 1. The sum of the probabilities for a given mode is not equal to one because of the cut described above and also because of the small number of gamma rays which convert in one of the anti-counters.

TABLE 1

Probability for seeing N gammas from a given decay mode

$$\eta^0 \rightarrow 2\gamma$$

N = 0	N = 1	N = 2
0.0819 ± 0.0041	0.3643 ± 0.0097	0.4688 ± 0.0114

$$\eta^0 \rightarrow \pi^0 \gamma\gamma$$

N = 0	N = 1	N = 2
0.0059 ± 0.0011	0.0803 ± 0.0040	0.2634 ± 0.0079

N = 3	N = 4
0.3459 ± 0.0093	0.1459 ± 0.0056

$$\eta^0 \rightarrow \pi^0$$

N = 0	N = 1	N = 2
0.0003 ± 0.0003	0.0135 ± 0.0016	0.0801 ± 0.0041

N = 3	N = 4	N = 5
0.2139 ± 0.0071	0.2808 ± 0.0084	0.1526 ± 0.0058

N = 6
0.0364 ± 0.0027

-more-

TABLE 1
continued

Background decay modes

$$2\pi^0 \rightarrow 4\gamma$$

N = 0	N = 1	N = 2
0.0087 ± 0.0017	0.0880 ± 0.0055	0.2594 ± 0.0101

N = 3	N = 4
0.2612 ± 0.0101	0.0976 ± 0.0058

$$3\pi^0 \rightarrow 6\gamma$$

N = 0	N = 1	N = 2
0.0007 ± 0.0005	0.0109 ± 0.0020	0.0962 ± 0.0063

N = 3	N = 4	N = 5
0.2159 ± 0.0100	0.2655 ± 0.0113	0.1496 ± 0.0081

N = 6
0.0382 ± 0.0039

Appendix E

This experiment was one of the last experiments to be done at the Cosmotron. Because of the inflexibility in the schedule we did not have the opportunity to test our experimental apparatus as thoroughly as we would have liked. Consequently, there were some characteristics of our equipment which we did not completely understand. Therefore, we would like to suggest certain areas which should be investigated and understood before using this or similar equipment again.

The single most important improvement to be made is with the measurement of the neutron time-of-flight. Our calibration of the neutron detector counter pairs had a resolution of approximately two nanoseconds in the time-of-flight to a given counter pair. A later measurement using three of the neutron detector counters and the same electronic logic found the resolution to be about 1/2 nanosecond for a given counter pair. (see Ref. 24). One difference between the two measurements was that the A-D circuitry was not used in the second measurement. This led us to believe that, despite our attempts to isolate it, there might have been noise getting into the A-D circuit.

Even with the large time resolution the neutron time-of-flight was sufficiently well determined so that events where etas were produced could be separated from events with faster times-of-flight such as charge exchange. Any improvement in the determination of the neutron time-of-flight would help the separation particularly for the faster

times-of-flight.

Another improvement would be to design the electronic logic
so that one knew which particular counter gave the timing signal.
In this experiment we knew which counter pair, but not which counter
of the pair, was responsible for the timing signal. While this lack
of knowledge was not serious in our case, causing an uncertainty of
approximately 1/2 nanosecond in the time-of-flight, it should be
possible to completely eliminate this uncertainty without unduly
complicating the electronic logic.

The anti-counter shield around the neutron detector should also
be improved. There was a considerable amount of material in the frame
which supported the neutron detector and the mirrors for the direct
and side views. The counters should have a better shield against
particles which originate in the steel frame and scatter into the de-
tector.

One topic which should be investigated is the distribution of
track lengths of the proton recoil in the neutron detector. Since we
determined the interaction point of the neutron by projecting the re-
coil proton track to the center plane of the counter in which it
began, the track must have at least two sparks. This meant that the
counters in the neutron detector must be thick enough so that the pro-
bability of the neutron interacting in the neutron detector was good,
but not so thick that the recoil proton was not energetic enough to
leave the counter. The thickness of the counters was chosen on the

basis of preliminary work done at the Cosmotron to optimize the detection efficiency for neutrons as a function of counter thickness (see Ref. 26). When we examined the distribution of track lengths of the recoil protons in the data, however, we found that the track lengths were shorter than expected. After looking at the data we would say that the counters should have been thinner.

Many of the problems associated with this experiment were connected with the operation of the neutron detector. While its performance was satisfactory, there is a question as to whether or not a simpler type of detector could do as well in determining the neutron time-of-flight and interaction point. For example, one should examine whether it is possible to achieve the desired spatial resolution on the interaction point of the neutron with a type of neutron detector such as the one used in Ref. 12. In that experiment a group of long cylinders of scintillator with phototubes on each end served as a neutron detector. The signals from the phototubes were used both for the neutron time-of-flight and for locating the interaction point in the scintillator. A detector of this type would be considerably simpler than ours since it would not have to be photographed and would not require the extensive electronics that our detector did. It might, however, be less efficient at detecting neutrons than our type of detector.

It would be better if the main spark chamber array were a complete 4π system. Such a system would greatly increase the probability for detecting all the gammas associated with a given event. Also

the chambers might be altered so that the first few plates were aluminum instead of steel. This would help to distinguish stopping charged prongs from short gammas which convert in the first few plates. Also it might be possible to get a good determination of the charged prong's direction from the sparks in the first few gaps of the large chambers. Something along this line would have to be done since it would not be possible to photograph the small chambers in a 4π system. Another possibility would be to replace the small chambers with wire spark chambers.

In our experiment the light pipe for the final beam defining counter located directly upstream from the target was long and had two curved sections near the end with the scintillator. The efficiency for transmitting light through such a pipe was not as good as for a short, straight light pipe and so the efficiency of the counter was less than it might have been. This inefficiency meant that we did not always get a good trigger when a good event occurred. In future work something should be done to increase the efficiency of this counter. Perhaps one of the small, new bialkali photocathode tubes could be attached to the counter, thus eliminating the need for a complicated light pipe.

If the momentum resolution of the incident beam could be considerably improved, then the angular region of the neutron detector in which neutrons produced in the reaction $\pi^- + p \rightarrow \eta^0 + n$ could interact would be very sharply defined. This would significantly increase the

signal-to-background level in the data.

REFERENCES

1. A. Pevsner et al., Phys. Rev. Letters 7, 421, (1961).

2. A. Rosenfeld et al., Rev. Mod. Phys. 40, 77 (1968).

3. D. Carmony, A. Rosenfeld, and R. De Walle, Phys. Rev. Letters 8, 117 (1962).

4. P. Bastien et al., Phys. Rev. Letters 8, 114 (1962).

5. M. Chretien et al., Phys. Rev. Letters 9, 127 (1962).

6. C. Alff et al., Phys. Rev. Letters 9, 322 (1962).

7. J. Bronzan and F. Low, Phys. Rev. Letters 12, 522 (1964).

8. L. Chan, Phys. Rev. 140, B1324 (1965).

9. G. Di Giugno et al., Phys. Rev. Letters 16, 767 (1966).

10. J. Grunhaus, Ph.D. Thesis (unpublished), Columbia University (1966).

11. M. Feldman et al., Phys. Rev. Letters 18, 868 (1967).

12. S. Buniatov et al., Phys. Letters 25B, 560 (1967).

13. F. Jacquet et al., Phys. Letters 25B, 574 (1967).

14. C. Baltay et al., Phys. Rev. Letters 19, 1495 (1967).

15. M. Wahlig et al., Phys. Rev. Letters 17, 221 (1967).

16. R. Cence et al., Phys. Rev. Letters 19, 1393 (1967).

17. Proceedings of the International Conference on Elementary Particles, Heidelberg, Germany, (1967).

18. R. Van Royen and V. Weisskopf, Il Nuovo Cimento 50A, 617 (1967).

19. C. Cavelli et al., Rev. Sci. Inst. 35, 1642 (1964). L. Guerriero et al., Rev. Sci. Inst. 37, 118 (1966).

20. D. Barton, Ph.D. Thesis (unpublished), M.I.T. (1968).

21. C. Schneider, M.S. Thesis (unpublished), M.I.T. (1964).

22. R. Hargraves, Ph.D. Thesis (unpublished), Brown University (1967).

23. F. Bulos et al., Submitted to the Physical Review (to be published).

24. Internal Report, "A Measurement of the Effective Refractive Index of Scintillator" by L. Kirkpatrick, L. Rosenson, and R. Thern, M.I.T., (1967).

25. NVERTX written by C. Bordner, A. Brenner, and F. Ronat at Harvard University. The experimental function was written by D. Barton, L. Kirkpatrick, B. Nelson, and R. Thern at M.I.T.

26. Internal Report, "Efficiency Determination for a Two-Module, Counter-Spark Chamber Neutron Detection System", by B. Kendall, and R. Lanou, Brown University, and D. Barton and L. Rosenson, M.I.T. (1966).
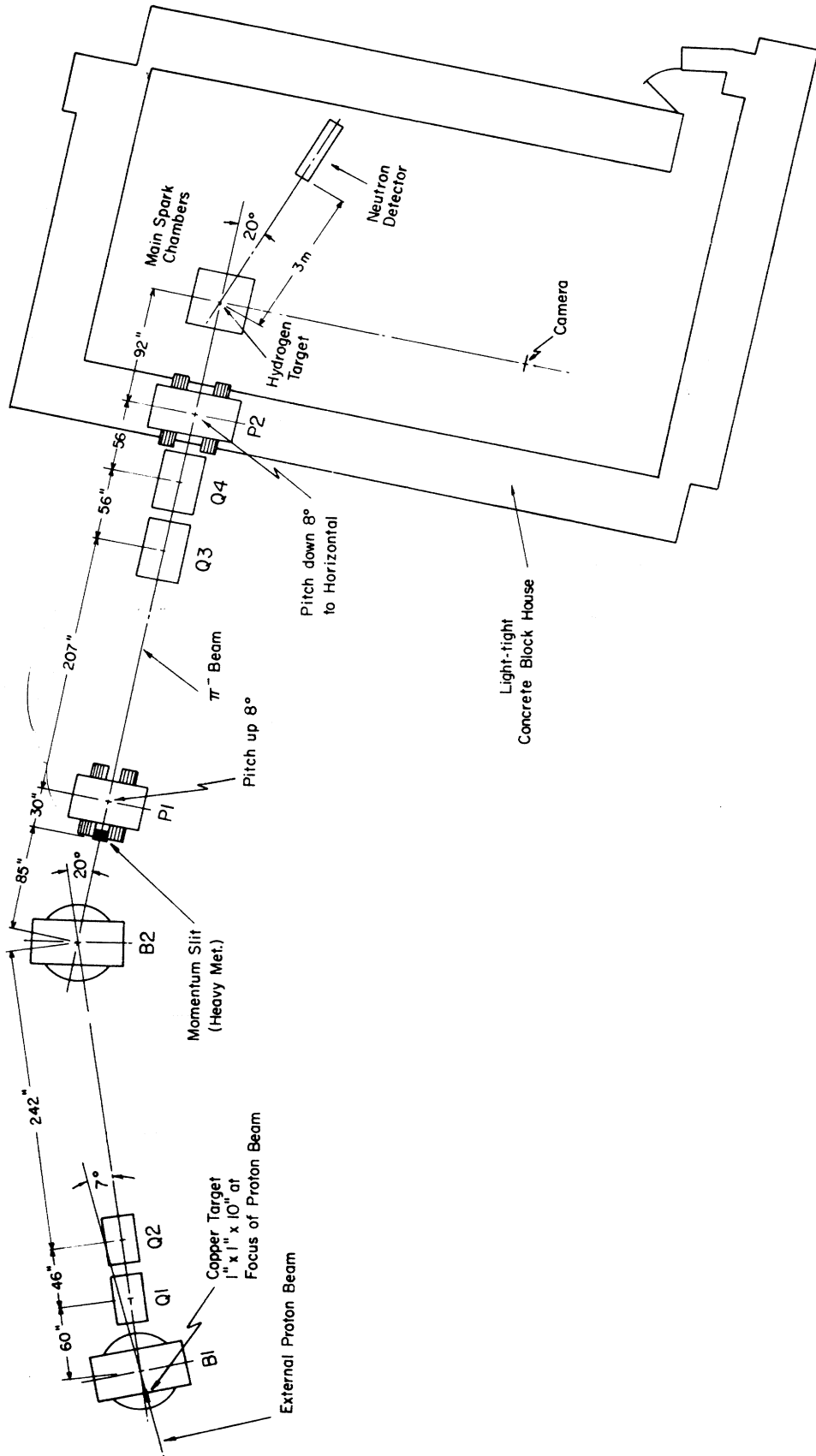
Figure 1. Beam Layout
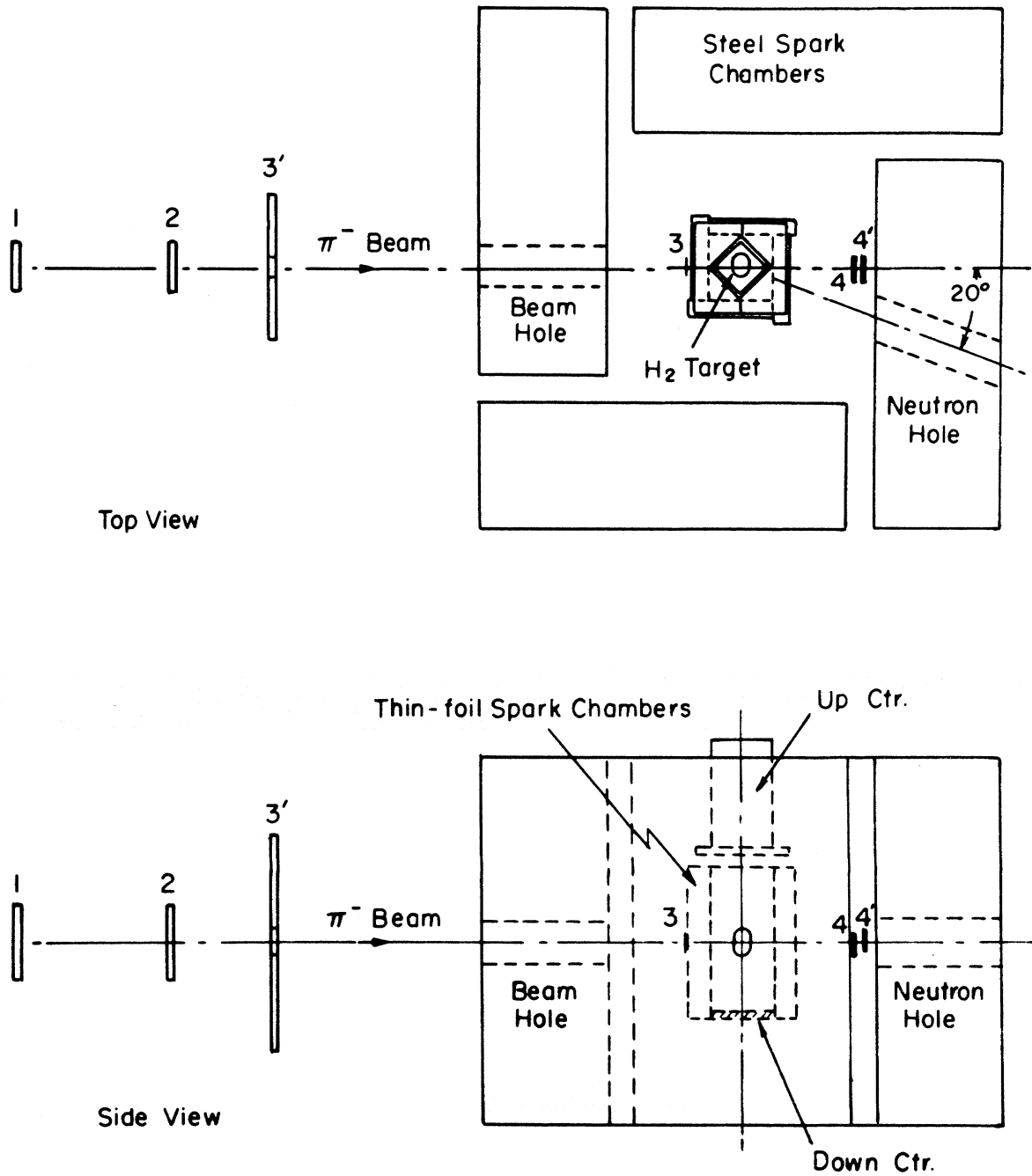
Figure 2. MAIN COUNTER AND SPARK CHAMBER ARRAY
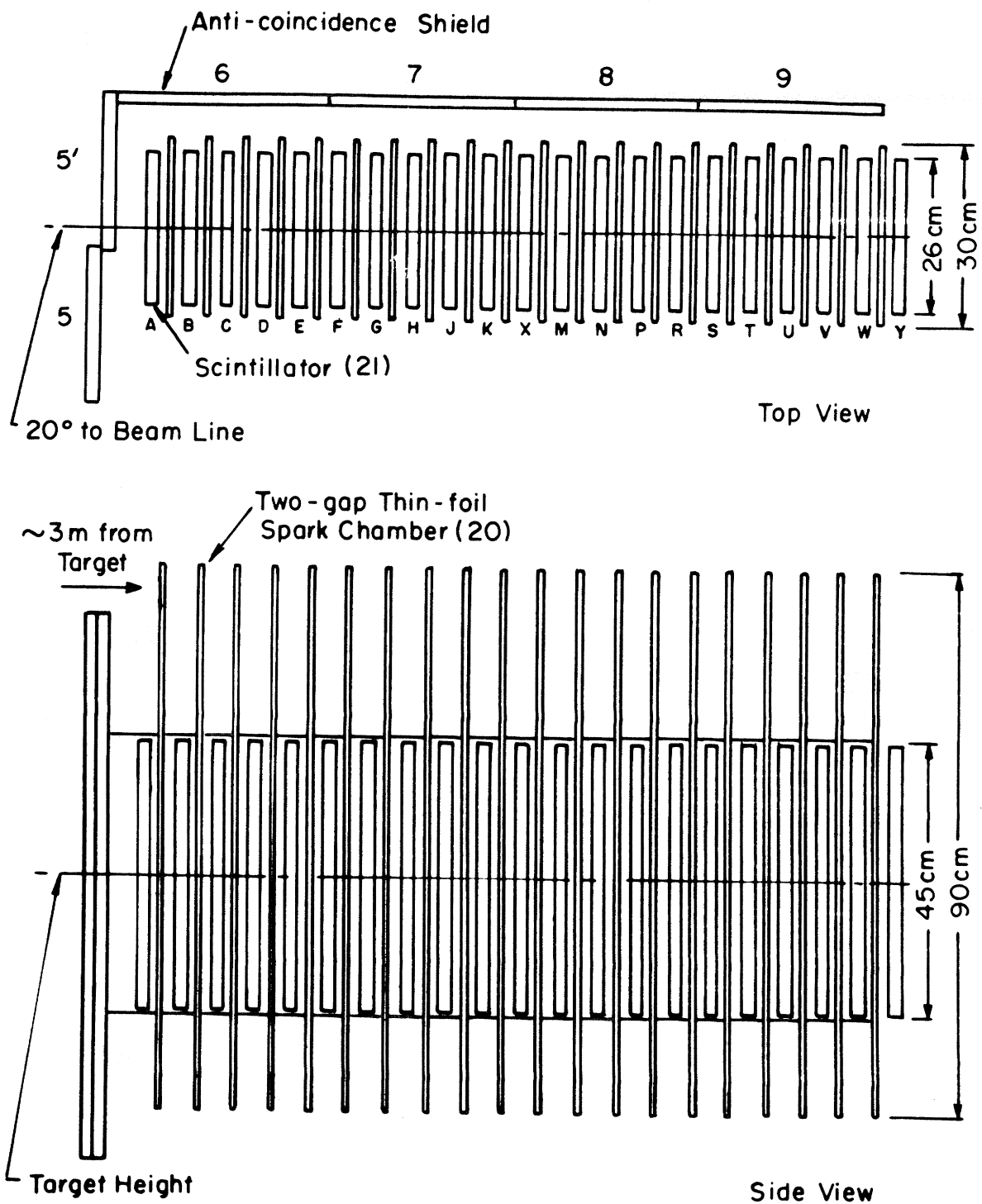
Figure 3. NEUTRON DETECTOR ARRAY

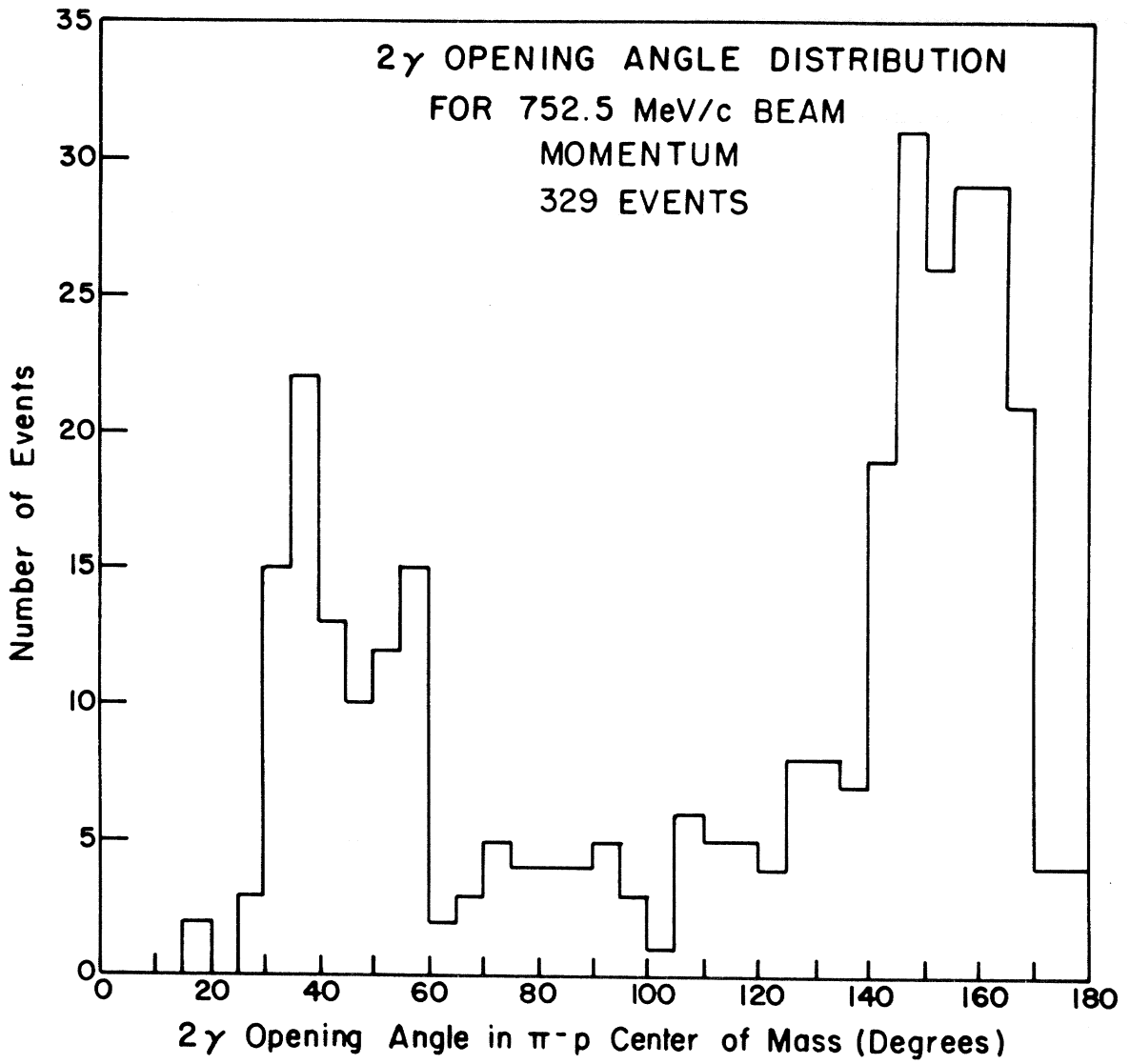SIDE
VIEW

BOTTOM
VIEW

TO CAMERA
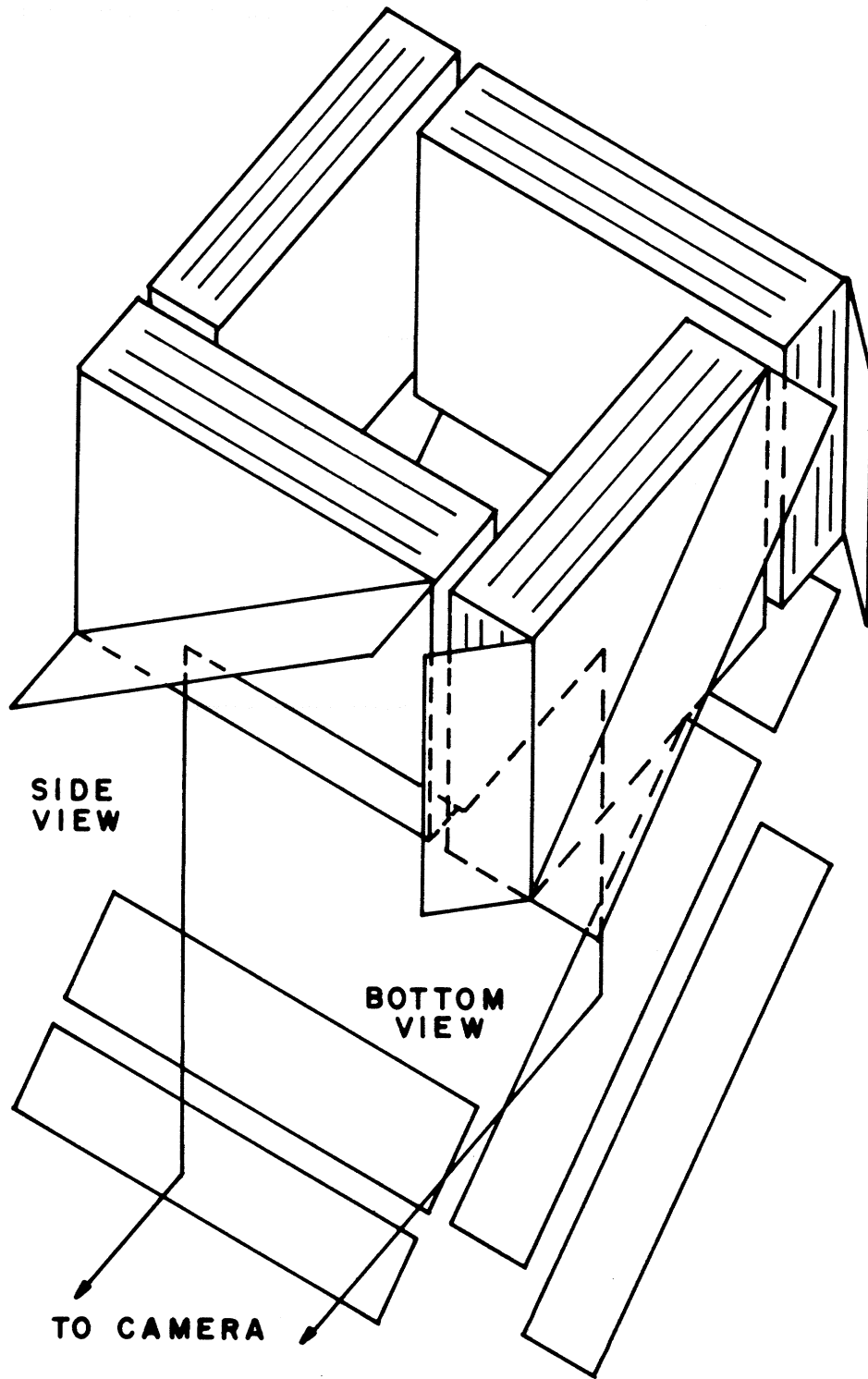
Figure 4. Optical System for Main Spark Chambers.

FIGURE 5
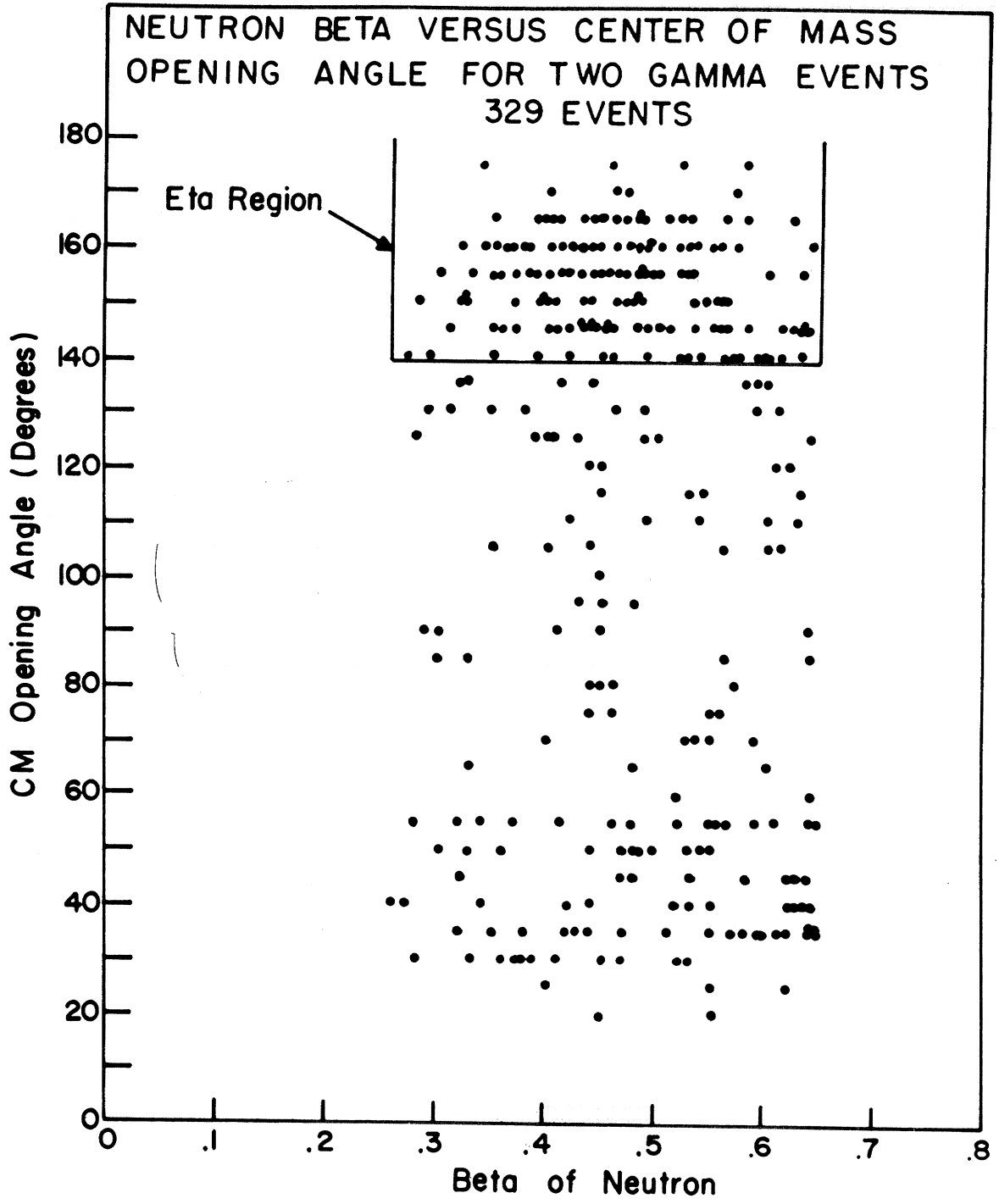
FIGURE 6

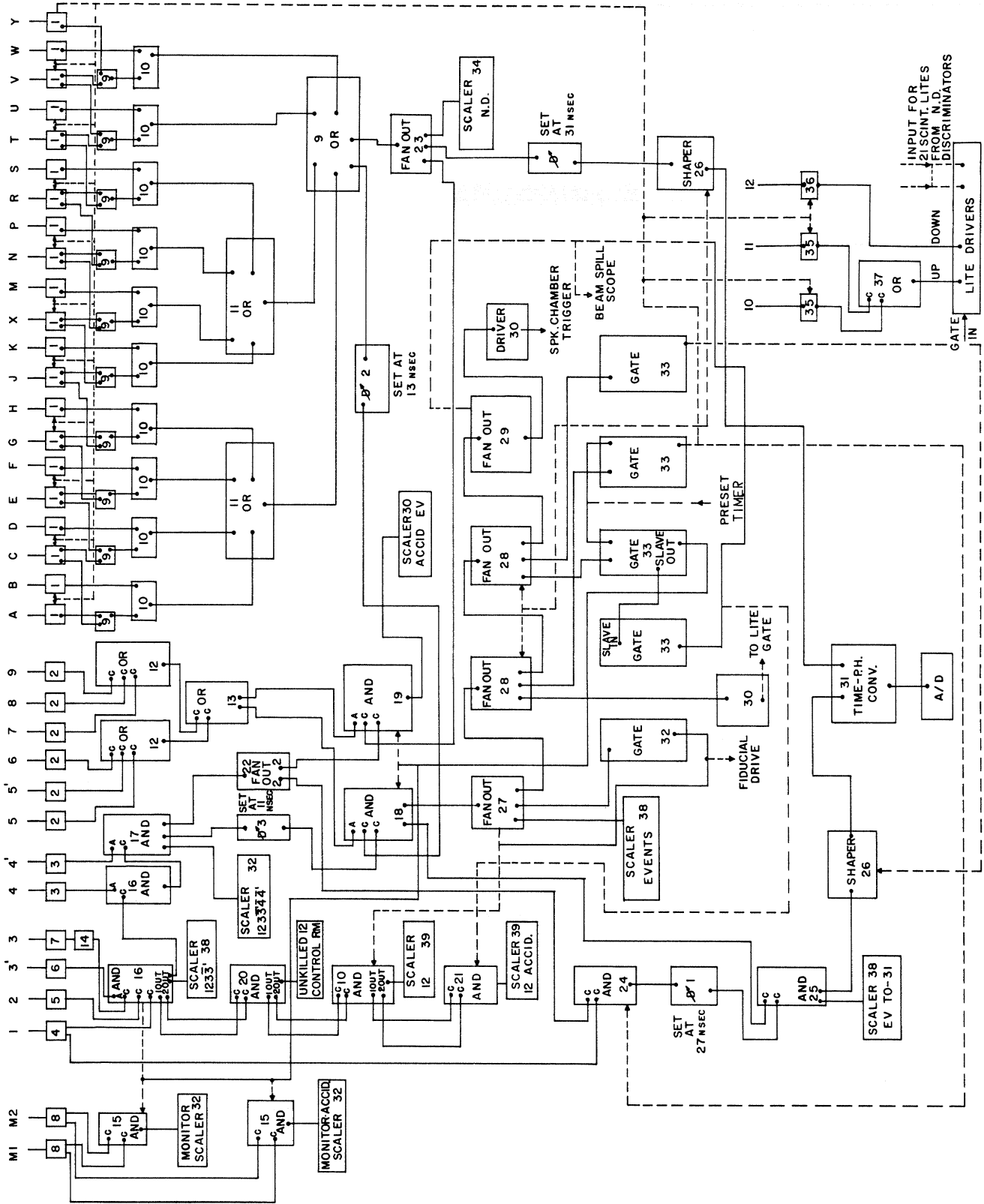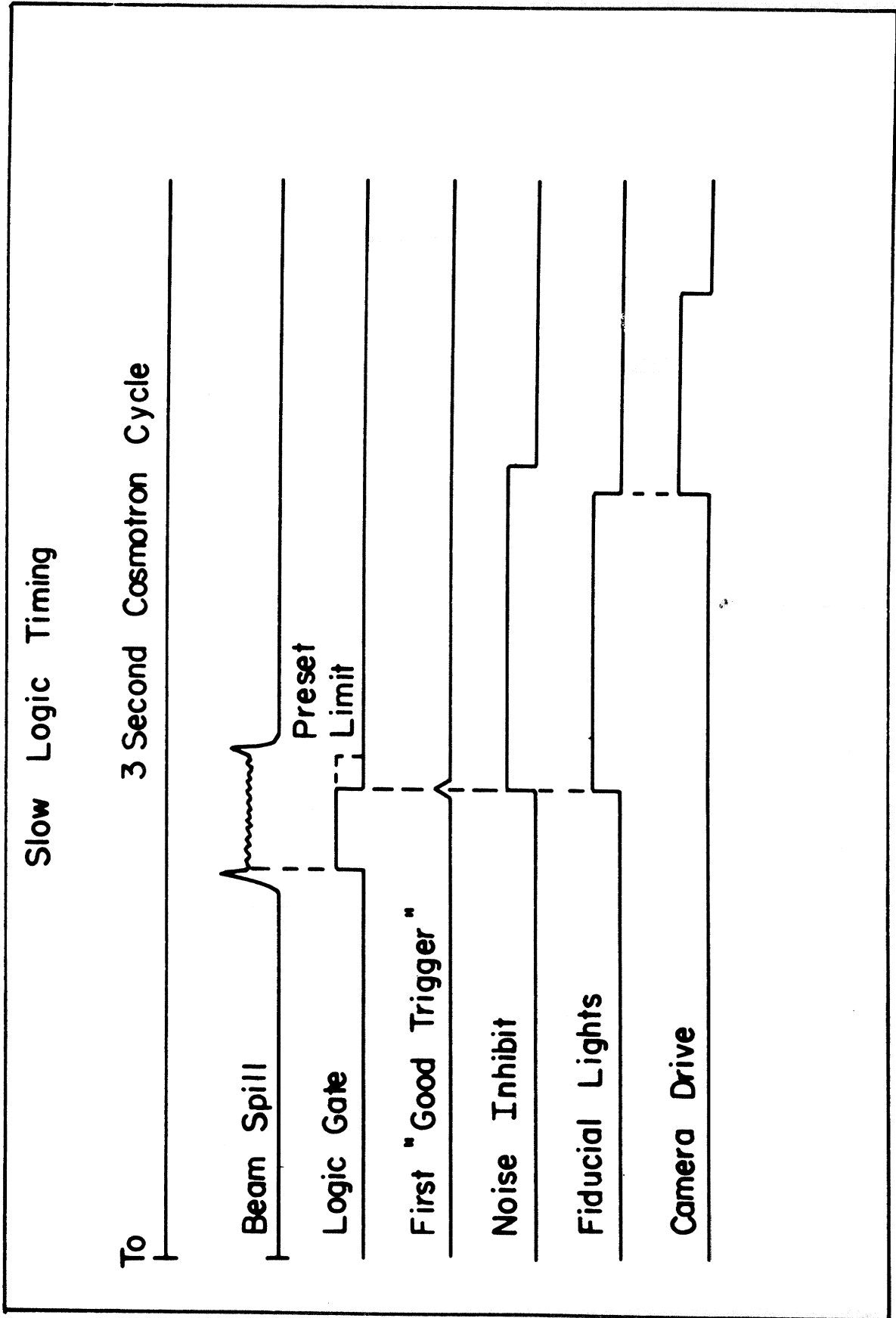FIGURE 7   ELECTRONIC   LOGIC

Slow Logic Timing

3 Second Cosmotron Cycle

To

Beam Spill

Logic Gate — Preset Limit
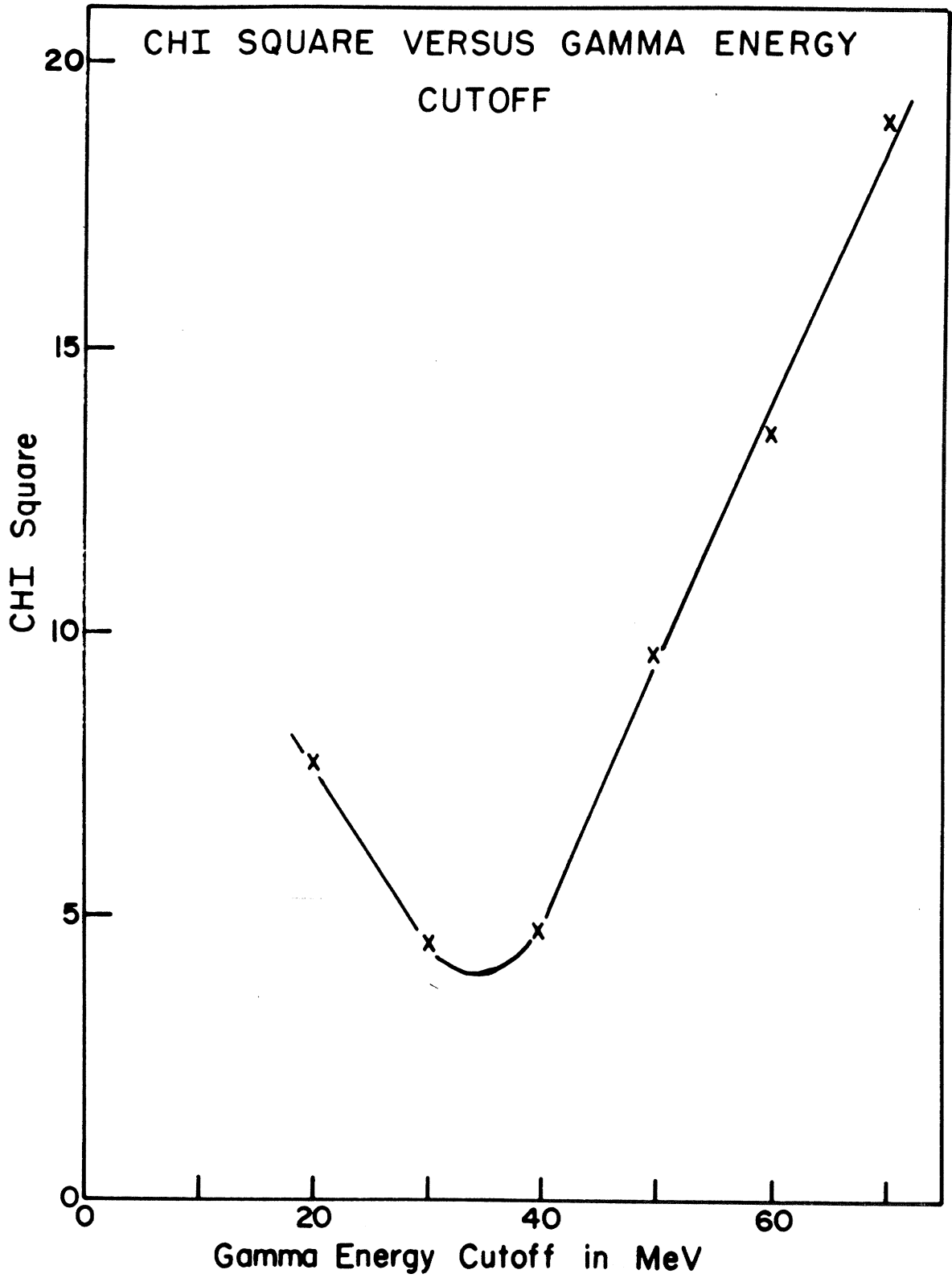
First "Good Trigger"
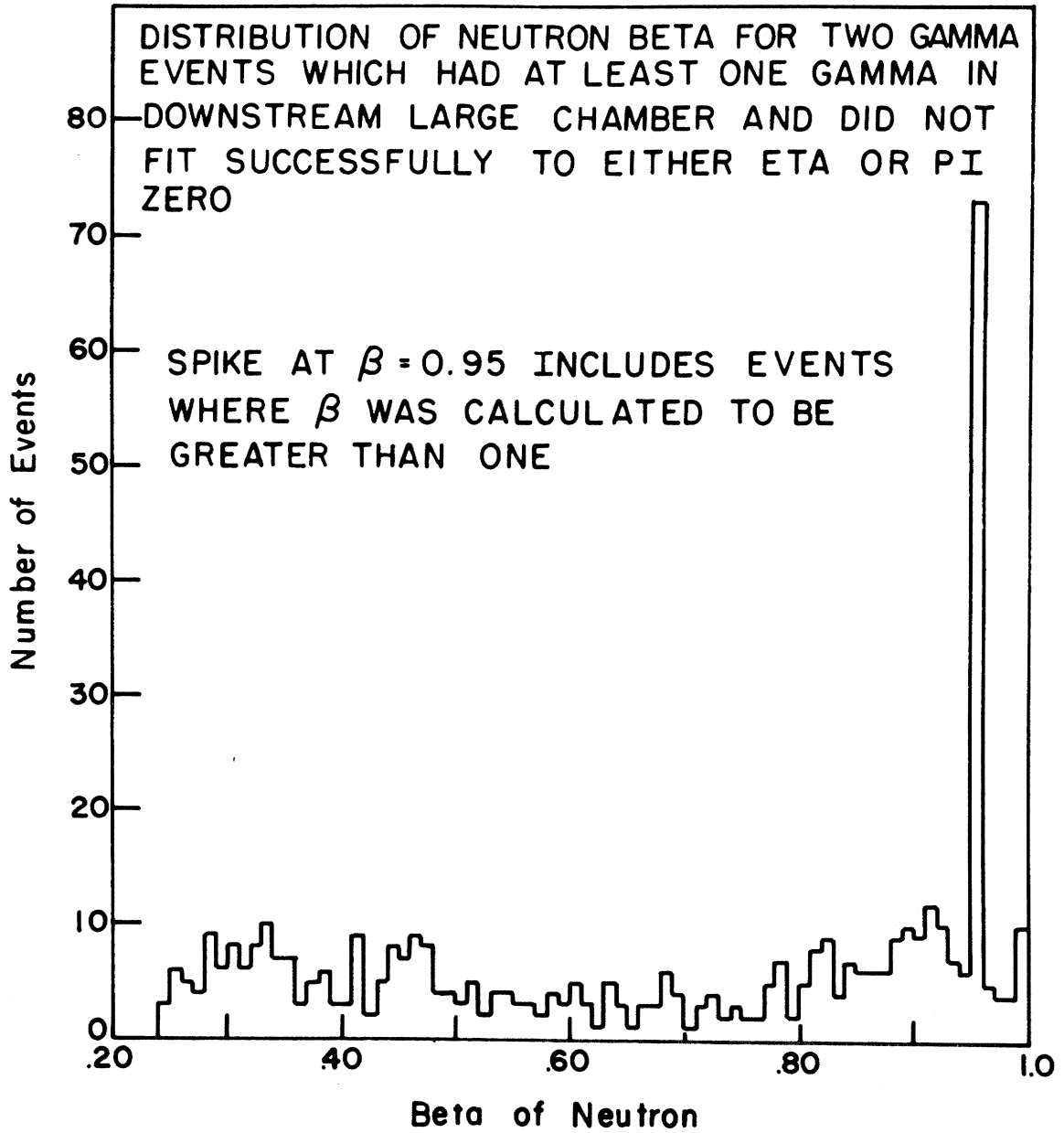
Noise Inhibit

Fiducial Lights

Camera Drive

FIGURE 8

FIGURE 9

DISTRIBUTION OF NEUTRON BETA FOR TWO GAMMA EVENTS WHICH HAD AT LEAST ONE GAMMA IN DOWNSTREAM LARGE CHAMBER AND DID NOT FIT SUCCESSFULLY TO EITHER ETA OR PI ZERO

SPIKE AT $\beta = 0.95$ INCLUDES EVENTS WHERE β WAS CALCULATED TO BE GREATER THAN ONE

FIGURE 10

DISTRIBUTION OF NEUTRON BETA FOR TWO GAMMA EVENTS WHICH HAD AT LEAST ONE GAMMA IN DOWNSTREAM LARGE CHAMBER BUT NOT WITHIN 4 cm OF NEUTRON DETECTOR HOLE AND WHICH DID NOT FIT SUCCESSFULLY TO EITHER ETA OR PI ZERO CONSTRAINT

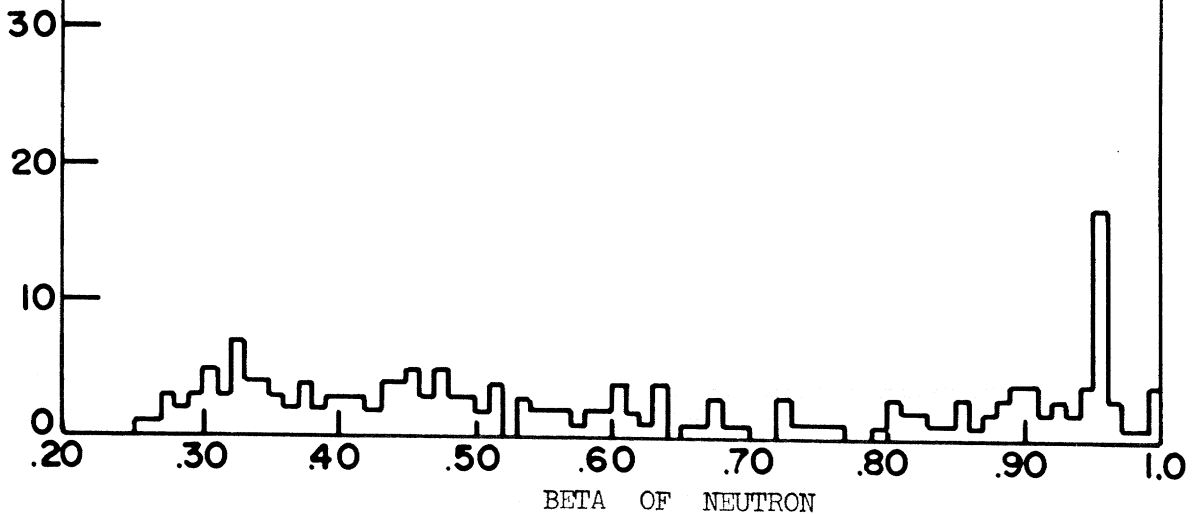SPIKE AT $\beta = 0.95$ INCLUDES EVENTS WHERE β WAS CALCULATED TO BE GREATER THAN ONE

BETA OF NEUTRON

FIGURE 11

NEUTRON TIME-OF-FLIGHT TO THE FIRST COUNTER IN THE NEUTRON DETECTOR VERSUS NEUTRON ANGLE IN THE LAB.

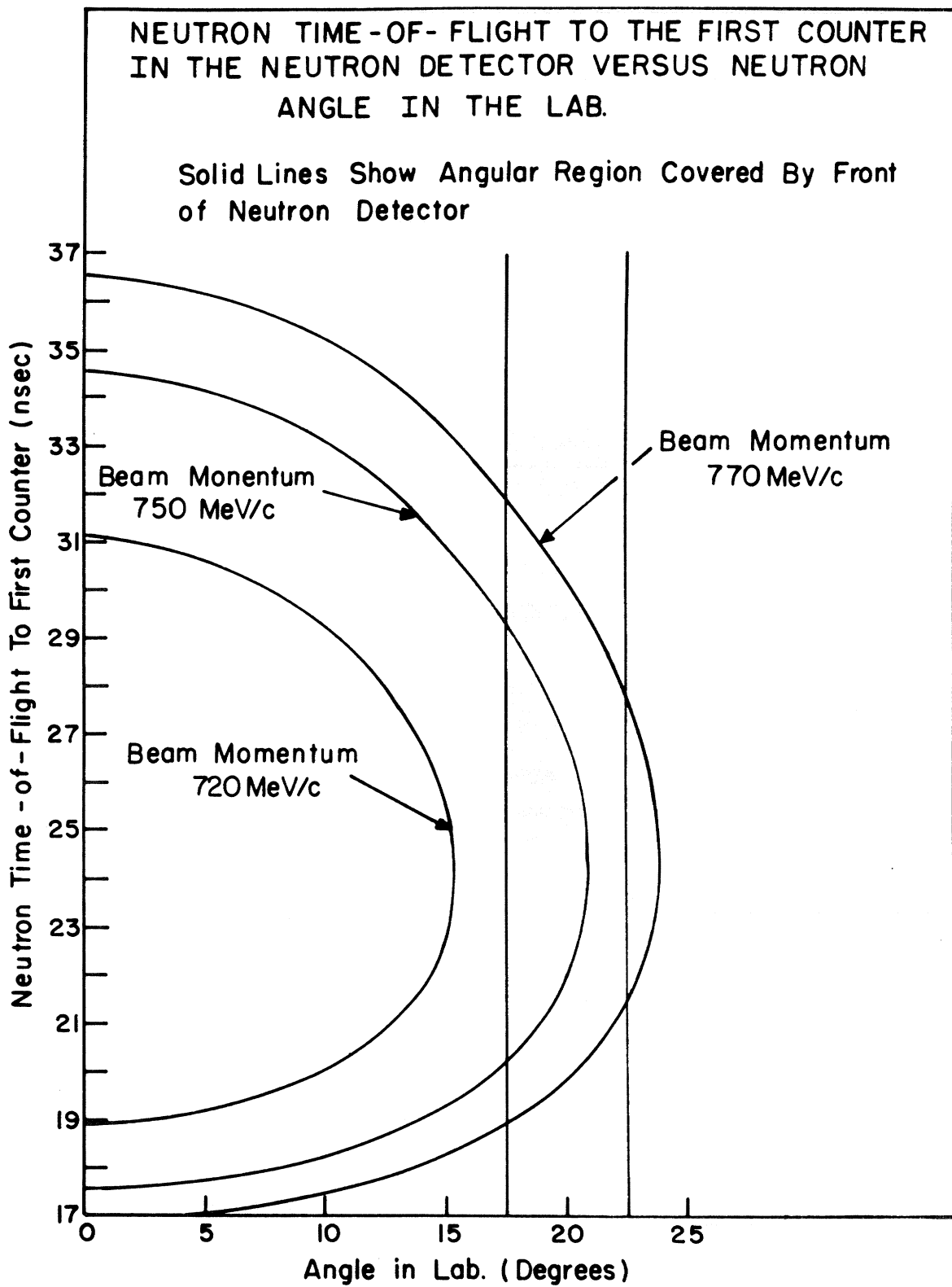Solid Lines Show Angular Region Covered By Front of Neutron Detector
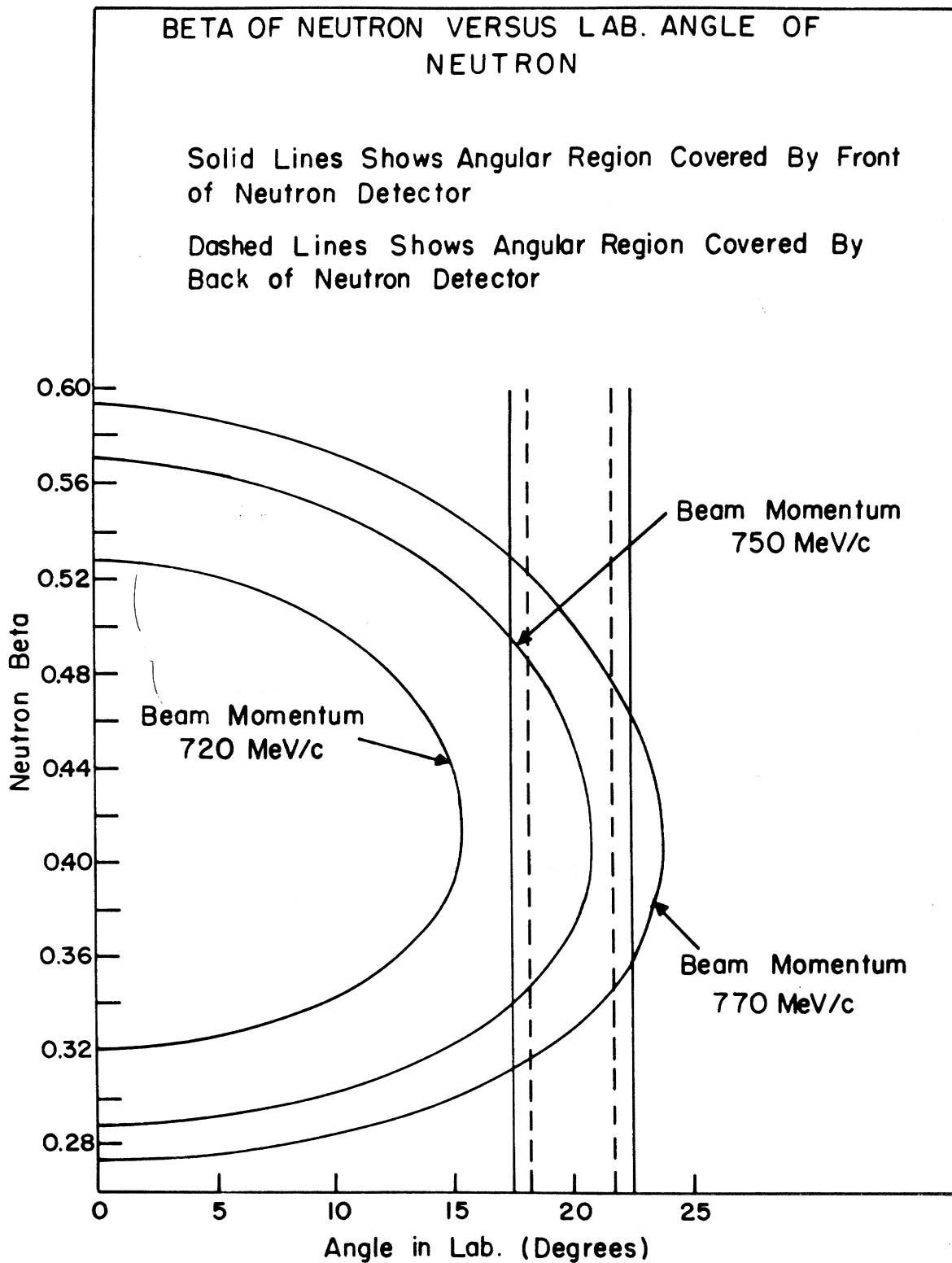
FIGURE 12

FIGURE 13

BIOGRAPHICAL NOTE

Bruce A. Nelson was born on June 8, 1938, in Columbus, Ohio. He attended public schools in Columbus and after graduation from Upper Arlington High School he entered M.I.T., where he majored in Physics. After receiving a B.S. degree from M.I.T. in 1961, he was employed by the Laboratory for Nuclear Science at M.I.T.. He became a graduate student in the Department of Physics at M.I.T. in 1964.